

Dissipative response of driven bead-spring-dashpot chains

R. Kailasham^{a)}

Department of Chemical Engineering, Indian Institute of Technology Indore, Khandwa Road, Simrol, Madhya Pradesh - 453552, India

(Dated: 9 July 2025)

The work dissipated in pulling a polymer chain with internal friction is numerically calculated by considering a sequence of N bead-spring-dashpots tethered at one end and being pulled at the other using a harmonic trap via linear and symmetric protocols. The variation of the dissipation with the chain length, pulling trap stiffness, and the internal friction parameter are examined in detail for both the protocols. In the limit of high trap stiffness: (i) the dissipation *decreases* with N for chains with internal friction, keeping all other parameters constant, and (ii) the relationship between the dissipation and internal friction parameter deviates from linearity as N is increased. Consequently, a closed-form expression between the dissipated work in driving a chain of spring-dashpots and the damping coefficient of a single dashpot can be written only for the case of $N = 1$ [as shown in Phys. Rev. Res. **2**, 013331 (2020)] and not for the general case of $N > 1$.

I. INTRODUCTION

The dynamics of conformational transitions in polymer molecules is governed not only by the solvent friction, but also by intramolecular interactions whose effects are collectively referred to as internal friction or internal viscosity^{1–28} (IV). The rheological consequences of internal friction^{1–6} include the appearance of a stress jump at the inception of shear flow⁷, and a non-vanishing dynamic viscosity in the high frequency limit⁸ of small amplitude oscillatory shear experiments. In the biophysical context, internal friction slows down of the reconfiguration or folding time of the molecule^{9–20}. While these two aspects of IV have received immense scrutiny, the mechanical or dissipative consequence of internal friction remains less thoroughly explored^{21–28}. The work dissipated in the forced uncoiling of condensed DNA globules^{22,26}, the viscoelastic response of single molecules of polysaccharides²³, ciliary oscillations in microorganisms²⁷, are all modulated by the presence of a frictional mechanism that is not hydrodynamic in nature. Given the wide range of contexts in which internal friction modulates the mechanical response of molecules, it is therefore essential to quantify the work required in subjecting polymer chains with internal friction to various driving protocols. In this paper, we address this knowledge gap by analytically deriving the appropriate expressions for a coarse-grained polymer model.

The concept of internal friction is an emergent phenomenon, and need not be invoked in an all-atom model of polymeric chains in which the interaction between various segments is specified completely in terms of bonded and non-bonded potentials^{29,30}. The process of coarse-graining such a detailed model into a chemistry-agnostic bead-spring chain model requires the inclusion of an additional frictional term^{31,32}. The mathematical form of the additional term to be included depends on whether one is

trying to model *wet* or *dry* internal friction³³. This classification is based on if the dissipation vanishes (*wet*) or persists (*dry*) in the extrapolated limit of zero solvent viscosity, respectively. The distinction is purely notional³⁰, and it is possible for a single polymer to possess both types of internal friction. Cohesive interactions between the segments of a polymer chain^{24,25,34} are known to result in *wet* internal friction, as discussed in Ref. 33. In a coarse-grained model, these interactions are represented using non-bonded potentials that operate between any two beads in the polymer. The scaling of the work dissipated due to wet internal friction as a function of the number of beads in the chain has been investigated in detail by Netz and coworkers^{24,25}. Resistance to dihedral angle rotation has been attributed as a source of *dry* internal friction^{10,16,17,32,35–37}, and is represented in coarse-grained models by the inclusion of a dashpot in parallel with each spring of a bead-spring-chain model^{1–4,38,39}. The challenge of developing a numerical algorithm to simulate a bead-spring-dashpot chain with greater than two beads is an arduous one, and has only been surmounted recently^{39,40}. For the simplest case of a dumbbell (two beads connected by a spring-dashpot arrangement) whose one bead is tethered, the damping coefficient of the dashpot has been shown to be the friction coefficient associated with pulling the free bead of the dumbbell over a fixed distance at a constant velocity, in the limit of zero solvent friction and large trap stiffness³³. This mechanical interpretation of dry internal friction allows for the prescription of a protocol for the estimation of internal friction coefficient of any polymer using single-molecule force spectroscopy experiments³³. Polymer chains are usually modeled as a chain of interconnected beads, to capture the multiple timescales associated with their dynamics^{41,42}, and a dumbbell model is therefore insufficient for several applications. An accurate coarse-grained description of polymers with dry internal friction would therefore require the knowledge of: (a) what the dissipation incurred in pulling a series of spring-dashpots is, and (b) how the dissipation of a bead-spring-dashpot chain is related to the damping co-

^{a)} Electronic mail: rkailasham@iiti.ac.in

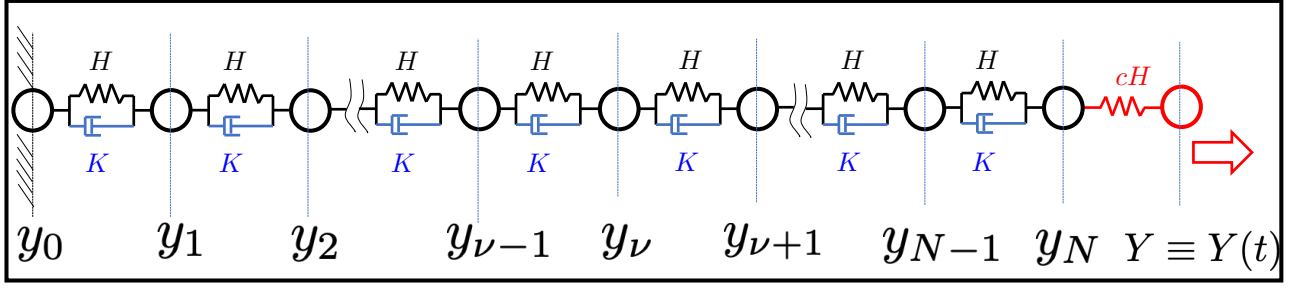


FIG. 1. A polymer chain with $N + 1$ beads, with one end (y_0) tethered and the other (y_N) connected to an optical/laser trap whose center $Y(t)$ moves according to a deterministic protocol. The spring-dashpot arrangement that connects adjacent beads is composed of a Hookean spring of stiffness H and a dashpot with damping coefficient K . The stiffness of the steering spring is given by cH , with $c > 0$. The motion of the N beads numbered y_1, y_2, \dots, y_N is governed by eq. (4).

efficient of a single dashpot. The present work addresses these two questions.

The work statistics of a Rouse chain whose one end is fixed and the other subjected to one-dimensional motion via pulling at a constant velocity or oscillation at a fixed frequency have been derived^{43–45}. We extend the approach to a bead-spring-dashpot chain, and derive expressions for the work statistics under both the protocols to answer (a). We discover, however, that the dependence of the dissipation of the number of spring-dashpots in the chain is highly non-trivial, and is dictated by the stiffness of the steering spring relative to that of a single spring in the chain. Essentially, a soft steering spring results in the dissipation increasing with N , while a stiff spring results in the dissipation decreasing with N . This surprising result precludes a straightforward to the question posed in (b) above.

This document is organized as follows. Section II derives the expression for the work dissipated in subjecting a tethered bead-spring-dashpot chain to an arbitrary pulling protocol. The case of constant velocity pulling and oscillatory driving are considered in Sec. III, and expressions for the work dissipated in these two protocols are derived. A comparison with previous work done in the field of dissipation calculation for driven Rouse chains is provided in Sec. IV, and Sec. V discusses the results of the present work for both the driving protocols. We conclude in Sec. VI. The appendix contains the derivation of identities used in the simplification of expressions appearing in Sections II and III.

II. GOVERNING EQUATIONS

A polymer chain with $(N + 1)$ beads is considered in the present work, with each bead of radius a connected to its nearest neighbor via a spring-dashpot arrangement as shown in Fig. 1. The polymer is suspended in a newtonian solvent of viscosity η_s at a temperature T and is confined to motion along a single dimension. The stiffness of each Hookean spring is H , and the damping coefficient of each dashpot is K . The positions of the beads are de-

noted by $[y_0, y_1, \dots, y_{N+1}]$. The first bead of the chain is kept fixed. The last bead is attached to an optical/laser trap of stiffness cH , where c is a positive constant, and the location of the trap $Y(t)$ is varied in time according to some protocol. The Hamiltonian of the system is therefore given by

$$\mathcal{H} = \frac{H}{2} \sum_{\nu=0}^{N-1} (y_{\nu+1} - y_{\nu})^2 + \frac{cH}{2} (Y(t) - y_N)^2 \quad (1)$$

Using the principles of polymer kinetic theory^{42,46}, and assuming the beads are massless, a force-balance may be written for the ν^{th} bead in the chain, by requiring that the sum of the drag force, spring force, internal friction (IV) force, and the Brownian force vanishes. The drag force, spring force and the Brownian force on the ν^{th} bead are given by $F_{\nu}^{\text{D}} = -\zeta \llbracket \dot{y}_{\nu} \rrbracket$, $F_{\nu}^{\text{S}} = -(\partial \mathcal{H} / \partial y_{\nu})$ and $F_{\nu}^{\text{B}} = -k_B T (\partial \ln \Psi / \partial y_{\nu})$, respectively, where, k_B is Boltzmann's constant, $\zeta = 6\pi\eta_s a$ the drag coefficient, $\llbracket \dots \rrbracket$ denotes a momentum-average, and $\Psi \equiv \Psi(y_1, \dots, y_N)$ is the configurational distribution function of the bead positions. The IV force on the ν^{th} that is not at the chain ends is written as follows⁴⁶

$$F_{\nu}^{\text{IV}} = K [y_{\nu+1} - 2y_{\nu} + y_{\nu-1}] \quad (2)$$

The equation of motion for the ν^{th} bead that is not at the chain ends may therefore be given by the following expression

$$\llbracket \dot{y}_{\nu} \rrbracket = -\frac{k_B T}{\zeta} \left(\frac{\partial \Psi}{\partial y_{\nu}} \right) - \frac{1}{\zeta} \left(\frac{\partial \mathcal{H}}{\partial y_{\nu}} \right) + \frac{1}{\zeta} F_{\nu}^{\text{IV}} \quad (3)$$

It is convenient to work with collective coordinates $\mathbf{y} \equiv [y_1, y_2, \dots, y_N]$, so that the equation of motion may be rewritten as follows

$$\llbracket \dot{\mathbf{y}} \rrbracket = -\frac{H}{\zeta} \mathbf{A} \cdot \mathbf{y} - \frac{K}{\zeta} \mathbf{L} \cdot \llbracket \dot{\mathbf{y}} \rrbracket + \frac{cH}{\zeta} \chi(t) - \frac{k_B T}{\zeta} \left(\frac{\partial \ln \Psi}{\partial \mathbf{y}} \right) \quad (4)$$

where $\chi(t) = [0, 0, \dots, Y(t)]$ represents the deterministic pulling-protocol applied to the steering bead; \mathbf{A} and \mathbf{L}

are symmetric tridiagonal $N \times N$ matrices whose elements are defined as follows

$$A_{jk} = \begin{cases} 2; & j = k \neq N \\ (c+1); & j = k = N \\ -1; & |j - k| = 1 \\ 0; & \text{otherwise} \end{cases} \quad (5)$$

$$L_{jk} = \begin{cases} 2; & j = k \neq N \\ 1; & j = k = N \\ -1; & |j - k| = 1 \\ 0; & \text{otherwise} \end{cases} \quad (6)$$

Note that \mathbf{A} becomes the standard Rouse matrix when the stiffness of the steering spring is the same as that of the springs in the polymer, i.e., for $c = 1$. Upon simplifying eq. (4),

$$[\dot{\mathbf{y}}] = -\frac{H}{\zeta} \mathbf{D} \cdot \mathbf{A} \cdot \mathbf{y} + \frac{cH}{\zeta} \mathbf{D} \cdot \boldsymbol{\chi}(t) - \frac{k_B T}{\zeta} \mathbf{D} \cdot \left(\frac{\partial \ln \Psi}{\partial \mathbf{y}} \right), \quad (7)$$

with

$$\mathbf{D} = [\boldsymbol{\delta} + \varphi \mathbf{L}]^{-1}. \quad (8)$$

where $\varphi = K/\zeta$ is the internal friction parameter. Substituting eq. (7) into the equation of continuity for the probability density in configuration space,

$$\frac{\partial \Psi}{\partial t} = -\frac{\partial}{\partial \mathbf{y}} \cdot \{[\dot{\mathbf{y}}] \Psi\} \quad (9)$$

we obtain the following Fokker-Planck equation

$$\begin{aligned} \frac{\partial \Psi}{\partial t} = & -\frac{\partial}{\partial \mathbf{y}} \cdot \left\{ \left[-\frac{H}{\zeta} \mathbf{D} \cdot \mathbf{A} \cdot \mathbf{y} + \frac{cH}{\zeta} \mathbf{D} \cdot \boldsymbol{\chi}(t) \right] \Psi \right\} \\ & + \frac{1}{2} \left(\frac{2k_B T}{\zeta} \right) \frac{\partial}{\partial \mathbf{y}} \frac{\partial}{\partial \mathbf{y}} : [\mathbf{D} \Psi], \end{aligned} \quad (10)$$

where we have made use of the fact that $(\partial/\partial \mathbf{y}) \cdot \mathbf{D} = 0$ since the diffusion tensor \mathbf{D} for the system is independent of bead positions. The stochastic differential equation equivalent to eq. (10) may be written using the Itô interpretation⁴¹ as follows

$$\begin{aligned} d\mathbf{y} = & \left[-\frac{H}{\zeta} \mathbf{D} \cdot \mathbf{A} \cdot \mathbf{y} + \frac{cH}{\zeta} \mathbf{D} \cdot \boldsymbol{\chi}(t) \right] dt \\ & + \sqrt{\frac{2k_B T}{\zeta}} \mathbf{B} \cdot d\mathbf{M}_t; \quad \mathbf{B} \cdot \mathbf{B}^T = \mathbf{D} \end{aligned} \quad (11)$$

where \mathbf{M}_t represents a Wiener process. The equivalent Langevin form of eq. (11) is given by

$$\frac{d\mathbf{y}}{dt} = \left(\frac{H}{\zeta} \right) [-\mathbf{D} \cdot \mathbf{A} \cdot \mathbf{y} + c\mathbf{D} \cdot \boldsymbol{\chi}(t)] + \sqrt{\frac{k_B T}{\zeta}} \boldsymbol{\eta}(t) \quad (12)$$

where the moments of the noise term $\boldsymbol{\eta}(t)$ obey

$$\langle \boldsymbol{\eta}(t) \rangle = 0; \quad \langle \boldsymbol{\eta}(t') \boldsymbol{\eta}(t'') \rangle = 2\mathbf{D} \delta(t' - t'') \quad (13)$$

Going forward, we use the length scale $l_H = \sqrt{k_B T/H}$ and time scale $t_s = \zeta/H$ to non-dimensionalize eq. (12) and obtain

$$\frac{d\mathbf{z}}{d\tau} = -\mathbf{D} \cdot \mathbf{A} \cdot \mathbf{z}(\tau) + \mathbf{D} \cdot \mathbf{h}(\tau) + \boldsymbol{\mu}(\tau) \quad (14)$$

where

$$\begin{aligned} \mathbf{z} = \mathbf{y}/l_H = \sqrt{H/k_B T} \mathbf{y}; \quad \alpha = Y/l_H = \sqrt{H/k_B T} Y; \\ \tau = Ht/\zeta; \quad \mathbf{h}(\tau) = [0, 0, \dots, c\alpha(\tau)] \end{aligned} \quad (15)$$

and the dimensionless noise term obeys

$$\langle \boldsymbol{\mu}(\tau) \rangle = 0; \quad (16)$$

and

$$\langle \boldsymbol{\mu}(\tau') \boldsymbol{\mu}(\tau'') \rangle = 2\mathbf{D} \delta(\tau' - \tau''). \quad (17)$$

The formal solution to eq. (14) is given by

$$\begin{aligned} \mathbf{z}(\tau) = & \mathbf{G}(\tau) \cdot \mathbf{z}(0) \\ & + \int_0^\tau d\tau' \mathbf{G}(\tau - \tau') \cdot [\mathbf{D} \cdot \mathbf{h}(\tau') + \boldsymbol{\mu}(\tau')] \end{aligned} \quad (18)$$

where

$$\mathbf{G}(\tau) = \exp[-\mathbf{D} \cdot \mathbf{A} \tau] \quad (19)$$

The Jarzynski work^{43,47} done over a time interval τ_m may be evaluated as follows,

$$W = \frac{W^*}{k_B T} = \frac{1}{k_B T} \int_0^{\tau_m} \frac{\partial \mathcal{H}}{\partial Y} \dot{Y} dt = c \int_0^{\tau_m} (\alpha - z_N) \dot{\alpha} d\tau, \quad (20)$$

giving

$$W = \frac{c}{2} [\alpha^2(\tau_m) - \alpha^2(0)] - \int_0^{\tau_m} d\tau \dot{\mathbf{h}}(\tau) \cdot \mathbf{z}(\tau) \quad (21)$$

Substituting eq. (18) into eq. (21), we obtain

$$W = \frac{c}{2} [\alpha^2(\tau_m) - \alpha^2(0)] - \int_0^{\tau_m} d\tau \dot{\mathbf{h}}(\tau) \cdot \left[\mathbf{G}(\tau) \cdot \mathbf{z}(0) + \int_0^\tau d\tau' \mathbf{G}(\tau - \tau') \cdot \mathbf{D} \cdot \mathbf{h}(\tau') + \int_0^\tau d\tau' \mathbf{G}(\tau - \tau') \cdot \boldsymbol{\mu}(\tau') \right] \quad (22)$$

A matrix representation of the Hamiltonian may be written as follows

$$\frac{\mathcal{H}}{k_B T} = \frac{1}{2} \mathbf{z} \cdot \mathbf{A} \cdot \mathbf{z} + \frac{c}{2} \alpha^2 - \mathbf{h} \cdot \mathbf{z} \quad (23)$$

Using eq. (23), the dimensionless partition function is evaluated as

$$\begin{aligned} \mathcal{Z} &= \int \exp \left[-\frac{\mathcal{H}}{k_B T} \right] d\mathbf{z} \\ &= \exp \left[-\frac{c\alpha^2}{2} \right] \int \exp \left[-\frac{1}{2} \mathbf{A} : \mathbf{z} \mathbf{z} + \mathbf{h} \cdot \mathbf{z} \right] d\mathbf{z} \end{aligned} \quad (24)$$

The integral in eq. (24) may be simplified using the identity E.3-7 in ref. 42 to obtain the following expression for the dimensionless partition function,

$$\mathcal{Z} = \frac{(2\pi)^{N/2}}{\sqrt{\det(\mathbf{A})}} \exp \left[-\frac{c\alpha^2}{2} + \frac{1}{2} \mathbf{h} \cdot \mathbf{A}^{-1} \cdot \mathbf{h} \right] \quad (25)$$

The dimensionless free energy is then obtained as follows

$$F[\alpha(\tau)] = -\ln \mathcal{Z} = \frac{c\alpha^2(\tau)}{2} - \frac{1}{2} \mathbf{h}(\tau) \cdot \mathbf{A}^{-1} \cdot \mathbf{h}(\tau) \quad (26)$$

after ignoring the constant terms. The dimensionless probability distribution function for the bead positions in the system is given by

$$\begin{aligned} \Psi(\mathbf{z}) &= \frac{1}{\mathcal{Z}} \exp \left[-\frac{\mathcal{H}}{k_B T} \right] \\ &= \frac{\sqrt{\det(\mathbf{A})}}{(2\pi)^{N/2}} \exp \left\{ -\frac{1}{2} \mathbf{z} \cdot \mathbf{A} \cdot \mathbf{z} - \frac{1}{2} \mathbf{h} \cdot \mathbf{A}^{-1} \cdot \mathbf{h} + \mathbf{h} \cdot \mathbf{z} \right\} \end{aligned} \quad (27)$$

The mean positions of the beads and their fluctuations may then be deduced as follows

$$\langle \mathbf{z} \rangle = \mathbf{A}^{-1} \cdot \mathbf{h} \quad (28)$$

$$\langle (\mathbf{z} - \langle \mathbf{z} \rangle) (\mathbf{z} - \langle \mathbf{z} \rangle) \rangle = \mathbf{A}^{-1} \quad (29)$$

Taking an ensemble average on both sides of eq. (22), the expression for the mean work is obtained as follows

$$\begin{aligned} \langle W \rangle &= \frac{c}{2} [\alpha^2(\tau_m) - \alpha^2(0)] \\ &\quad - \int_0^{\tau_m} d\tau \dot{\mathbf{h}}(\tau) \cdot \mathbf{G}(\tau) \cdot \mathbf{A}^{-1} \cdot \mathbf{h}(0) \\ &\quad - \int_0^{\tau_m} d\tau \dot{\mathbf{h}}(\tau) \cdot \int_0^\tau d\tau' \cdot \mathbf{G}(\tau - \tau') \cdot \mathbf{D} \cdot \mathbf{h}(\tau') \end{aligned} \quad (30)$$

where we have used eq. (28) and the fact that the ensemble-average of the dimensionless noise term vanishes (cf. eq. (16)). The last term on the RHS of eq. (30) is simplified using integration by parts as shown in eqs. (A.1) - (A.4) of Appendix to obtain

$$\begin{aligned} \langle W \rangle &= \frac{c}{2} [\alpha^2(\tau_m) - \alpha^2(0)] - \int_0^{\tau_m} d\tau \dot{\mathbf{h}}(\tau) \cdot \mathbf{A}^{-1} \cdot \mathbf{h}(\tau) \\ &\quad + \int_0^{\tau_m} d\tau \int_0^\tau d\tau' \dot{\mathbf{h}}(\tau) \cdot \mathbf{G}(\tau - \tau') \cdot \mathbf{A}^{-1} \cdot \dot{\mathbf{h}}(\tau') \end{aligned} \quad (31)$$

Simplifying the last term on the RHS of eq. (31) using integration by parts as shown in eqs. (A.5) - (A.7) of Appendix results in

$$\begin{aligned} \langle W \rangle &= \left[\frac{c}{2} \alpha^2(\tau_m) - \frac{1}{2} \mathbf{h}(\tau_m) \cdot \mathbf{A}^{-1} \cdot \mathbf{h}(\tau_m) \right] \\ &\quad - \left[\frac{c}{2} \alpha^2(0) - \frac{1}{2} \mathbf{h}(0) \cdot \mathbf{A}^{-1} \cdot \mathbf{h}(0) \right] \\ &\quad + \int_0^{\tau_m} d\tau \int_0^\tau d\tau' \dot{\mathbf{h}}(\tau) \cdot \mathbf{G}(\tau - \tau') \cdot \mathbf{A}^{-1} \cdot \dot{\mathbf{h}}(\tau'). \end{aligned} \quad (32)$$

Recognizing that the first two terms on the RHS of the above equation represent the free-energy difference for the transition between the initial and final states (cf. eq. (26)), we may write

$$\langle W \rangle = \Delta F + \langle W_{\text{dis}} \rangle \quad (33)$$

where

$$\Delta F = F[\alpha(\tau_m)] - F[\alpha(0)], \quad (34)$$

and

$$\langle W_{\text{dis}} \rangle = \int_0^{\tau_m} d\tau \int_0^\tau d\tau' \dot{\mathbf{h}}(\tau) \cdot \mathbf{G}(\tau - \tau') \cdot \mathbf{A}^{-1} \cdot \dot{\mathbf{h}}(\tau') \quad (35)$$

We have therefore identified, in eq. (33), the reversible and irreversible (dissipative) components of the total average work done during the transition. We proceed to calculate the variance associated with the work process,

defined as

$$\sigma^2 = \langle (W - \langle W \rangle)^2 \rangle \quad (36)$$

Subtracting eq. (30) from eq. (22) and simplifying, we obtain

$$W - \langle W \rangle = - \int_0^{\tau_m} d\tau \dot{\mathbf{h}}(\tau) \cdot \mathbf{G}(\tau) \cdot [\mathbf{z}(0) - \langle \mathbf{z}(0) \rangle] - \int_0^{\tau_m} d\tau \int_0^\tau d\tau' \dot{\mathbf{h}}(\tau) \cdot \mathbf{G}(\tau - \tau') \cdot \boldsymbol{\mu}(\tau') \quad (37)$$

We may therefore use eq. (37) to calculate σ^2 as follows

$$\begin{aligned} \sigma^2 = & \int_0^{\tau_m} d\tau_1 \int_0^{\tau_m} d\tau_2 \dot{\mathbf{h}}(\tau_1) \cdot \mathbf{G}(\tau_1) \cdot \langle (\mathbf{z}(0) - \langle \mathbf{z}(0) \rangle) (\mathbf{z}(0) - \langle \mathbf{z}(0) \rangle) \rangle \cdot \mathbf{G}(\tau_2) \cdot \dot{\mathbf{h}}(\tau_2) \\ & + \int_0^{\tau_m} d\tau_1 \int_0^{\tau_1} d\tau'_1 \int_0^{\tau_m} d\tau_2 \int_0^{\tau_2} d\tau'_2 \dot{\mathbf{h}}(\tau_1) \cdot \mathbf{G}(\tau_1 - \tau'_1) \cdot \underline{\langle \boldsymbol{\mu}(\tau'_1) \boldsymbol{\mu}(\tau'_2) \rangle} \cdot \mathbf{G}(\tau_2 - \tau'_2) \cdot \dot{\mathbf{h}}(\tau_2) \end{aligned} \quad (38)$$

Using eqs. (29) and (17) to simplify the dash- and solid-underlined terms, respectively, on the RHS of eq. (38), we obtain

$$\begin{aligned} \sigma^2 = & \int_0^{\tau_m} d\tau_1 \int_0^{\tau_m} d\tau_2 \dot{\mathbf{h}}(\tau_1) \cdot \mathbf{G}(\tau_1) \cdot \mathbf{A}^{-1} \cdot \mathbf{G}(\tau_2) \cdot \dot{\mathbf{h}}(\tau_2) \\ & + 2 \int_0^{\tau_m} d\tau_1 \int_0^{\tau_1} d\tau'_1 \int_0^{\tau_m} d\tau_2 \int_0^{\tau_2} d\tau'_2 \dot{\mathbf{h}}(\tau_1) \cdot \mathbf{G}(\tau_1 - \tau'_1) \cdot \mathbf{D} \delta(\tau'_1 - \tau'_2) \cdot \mathbf{G}(\tau_2 - \tau'_2) \cdot \dot{\mathbf{h}}(\tau_2) \end{aligned} \quad (39)$$

Performing the integral over τ'_1 in the second term on the RHS of eq. (39),

$$\begin{aligned} \sigma^2 = & \int_0^{\tau_m} d\tau_1 \int_0^{\tau_m} d\tau_2 \dot{\mathbf{h}}(\tau_1) \cdot \mathbf{G}(\tau_1) \cdot \mathbf{A}^{-1} \cdot \mathbf{G}(\tau_2) \cdot \dot{\mathbf{h}}(\tau_2) \\ & + 2 \int_0^{\tau_m} d\tau_1 \int_0^{\tau_m} d\tau_2 \int_0^{\tau_2} d\tau'_2 \dot{\mathbf{h}}(\tau_1) \cdot \mathbf{G}(\tau_1 - \tau'_2) \cdot \mathbf{D} \cdot \mathbf{G}(\tau_2 - \tau'_2) \cdot \dot{\mathbf{h}}(\tau_2) \end{aligned} \quad (40)$$

Using the following identity (derived in Appendix 3)

$$\int_0^{\tau_2} d\tau'_2 \mathbf{G}(\tau_1 - \tau'_2) \cdot \mathbf{D} \cdot \mathbf{G}(\tau_2 - \tau'_2) = \frac{1}{2} \mathbf{A}^{-1} \cdot \mathbf{G}(\tau_1 - \tau_2) - \frac{1}{2} \mathbf{G}(\tau_1) \cdot \mathbf{A}^{-1} \cdot \mathbf{G}(\tau_2) \quad (41)$$

to simplify the second term on the RHS of eq. (40), we obtain

$$\begin{aligned} \sigma^2 = & \int_0^{\tau_m} d\tau_1 \int_0^{\tau_m} d\tau_2 \dot{\mathbf{h}}(\tau_1) \cdot \mathbf{A}^{-1} \cdot \mathbf{G}(\tau_1 - \tau_2) \cdot \dot{\mathbf{h}}(\tau_2) \\ = & 2 \int_0^{\tau_m} d\tau_1 \int_0^{\tau_1} d\tau_2 \dot{\mathbf{h}}(\tau_1) \cdot \mathbf{A}^{-1} \cdot \mathbf{G}(\tau_1 - \tau_2) \cdot \dot{\mathbf{h}}(\tau_2) \end{aligned} \quad (42)$$

From eqs. (35) and (42), we have

$$\sigma^2 = 2 \langle W_{\text{dis}} \rangle \quad (43)$$

which is expected for a Gaussian work distribution^{43,47}.

III. WORK CALCULATION

In this section, we calculate the work dissipated in driving the chain under two protocols that are commonly used in single-molecule force experiments^{48–52}. One manoeuvre involves moving the trap position at a constant velocity over a fixed distance. We refer to this interchangeably as the constant velocity pulling or the linear

protocol. The other method for driving the chain involves changing the trap position in a periodic manner. This is referred to as either the oscillatory driving or the symmetric protocol.

A. Constant velocity pulling (linear protocol)

We now evaluate the work statistics associated with a constant velocity pulling process, given by

$$\alpha(\tau) = \alpha(0) + v\tau \quad (44)$$

that acts over the interval $[0, \tau_m]$, such that the final bead is pulled over a dimensionless distance $[\alpha(\tau_m) - \alpha(0)] \equiv d = v\tau_m$ in the process. From the definition of $\mathbf{h}(\tau)$ in eq. (15) and the protocol defined in eq. (44), we may write

$$\mathbf{h}(\tau) = [0, 0, \dots, cv\tau]; \dot{\mathbf{h}}(\tau) = [0, 0, \dots, cv] \quad (45)$$

The vectors in eq. (45) are of length N each. Substituting these values into the expression for dissipated work given

by eq. (35),

$$\begin{aligned} \langle W_{\text{dis}} \rangle &= \int_0^{\tau_m} d\tau \int_0^\tau d\tau' \dot{\mathbf{h}}(\tau) \cdot \mathbf{G}(\tau - \tau') \cdot \mathbf{A}^{-1} \cdot \dot{\mathbf{h}}(\tau') \\ &= c^2 v^2 \int_0^{\tau_m} d\tau \int_0^\tau d\tau' [\mathbf{G}(\tau - \tau') \cdot \mathbf{A}^{-1}]_{NN}, \end{aligned} \quad (46)$$

where $[\dots]_{NN}$ denotes a matrix element. The inner-most integral on the RHS of eq. (46) may be processed as follows. Recognizing that

$$\frac{d}{d\tau'} \mathbf{A}^{-1} \cdot \mathbf{D}^{-1} \cdot \mathbf{G}(\tau - \tau') \cdot \mathbf{A}^{-1} = \mathbf{G}(\tau - \tau') \cdot \mathbf{A}^{-1}, \quad (47)$$

we may write

$$\begin{aligned} &\int_0^\tau d\tau' [\mathbf{G}(\tau - \tau') \cdot \mathbf{A}^{-1}]_{NN} \\ &= \int_0^\tau d\tau' \left\{ \frac{d}{d\tau'} \mathbf{A}^{-1} \cdot \mathbf{D}^{-1} \cdot \mathbf{G}(\tau - \tau') \cdot \mathbf{A}^{-1} \right\}_{NN} \\ &= [\mathbf{A}^{-1} \cdot \mathbf{D}^{-1} \cdot \mathbf{A}^{-1} - \mathbf{A}^{-1} \cdot \mathbf{D}^{-1} \cdot \mathbf{G}(\tau) \cdot \mathbf{A}^{-1}]_{NN} \end{aligned} \quad (48)$$

Plugging eq. (48) into eq. (46), we get

$$\begin{aligned} \langle W_{\text{dis}} \rangle &= c^2 v^2 \int_0^{\tau_m} d\tau \left[\mathbf{A}^{-1} \cdot \mathbf{D}^{-1} \cdot \mathbf{A}^{-1} - \mathbf{A}^{-1} \cdot \mathbf{D}^{-1} \cdot \mathbf{G}(\tau) \cdot \mathbf{A}^{-1} \right]_{NN} \\ &= c^2 v^2 \tau_m [\mathbf{A}^{-1} \cdot \mathbf{D}^{-1} \cdot \mathbf{A}^{-1}]_{NN} - c^2 v^2 \int_0^{\tau_m} d\tau [\mathbf{A}^{-1} \cdot \mathbf{D}^{-1} \cdot \mathbf{G}(\tau) \cdot \mathbf{A}^{-1}]_{NN} \end{aligned} \quad (49)$$

Recognizing that

$$\int_0^{\tau_m} d\tau [\mathbf{A}^{-1} \cdot \mathbf{D}^{-1} \cdot \mathbf{G}(\tau) \cdot \mathbf{A}^{-1}]_{NN} = - \left[\mathbf{A}^{-1} \cdot \mathbf{D}^{-1} \cdot [\exp(-\mathbf{D} \cdot \mathbf{A} \tau_m) - \delta] \cdot \mathbf{A}^{-1} \cdot \mathbf{D}^{-1} \cdot \mathbf{A}^{-1} \right]_{NN} \quad (50)$$

and combining eqs. (49) and (50), one obtains the following expression

$$\langle W_{\text{dis}} \rangle = \frac{c^2 d^2}{\tau_m} \left\{ \mathbf{A}^{-1} \cdot \mathbf{D}^{-1} \cdot \mathbf{A}^{-1} + \frac{1}{\tau_m} (\mathbf{A}^{-1} \cdot \mathbf{D}^{-1}) \cdot [\exp(-\mathbf{D} \cdot \mathbf{A} \tau_m) - \delta] \cdot \mathbf{A}^{-1} \cdot (\mathbf{D}^{-1} \cdot \mathbf{A}^{-1}) \right\}_{NN} \quad (51)$$

B. Oscillatory driving (symmetric protocol)

We next calculate the work done in oscillatory driving, i.e., assuming that the trap location is moved according to

$$\alpha(\tau) = \alpha(0) + d \sin(\omega\tau) \quad (52)$$

such that the trap location moves a dimensionless distance of d in a dimensionless time interval of τ_m . This

requires

$$\alpha(\tau_m) - \alpha(0) = d \sin(\omega\tau_m) = d \implies \omega = \pi/(2\tau_m). \quad (53)$$

We therefore have

$$\mathbf{h}(\tau) = [0, 0, \dots, c\alpha(\tau)]; \dot{\mathbf{h}}(\tau) = [0, 0, \dots, cd\omega \cos(\omega\tau)] \quad (54)$$

Substituting the above pulling protocol into the expression for dissipated work given by eq. (35),

$$\langle W_{\text{dis}} \rangle = \int_0^{\tau_m} d\tau \int_0^\tau d\tau' \dot{\mathbf{h}}(\tau) \cdot \mathbf{G}(\tau - \tau') \cdot \mathbf{A}^{-1} \cdot \dot{\mathbf{h}}(\tau') = c^2 d^2 \omega^2 \int_0^{\tau_m} d\tau \cos(\omega\tau) \int_0^\tau d\tau' [\cos(\omega\tau') \mathbf{G}(\tau - \tau') \cdot \mathbf{A}^{-1}]_{NN} \quad (55)$$

The innermost integral is evaluated as follows

$$\begin{aligned} \int_0^\tau d\tau' [\cos(\omega\tau') \mathbf{G}(\tau - \tau') \cdot \mathbf{A}^{-1}]_{NN} &= \frac{1}{\omega} [\sin(\omega\tau') \mathbf{G}(\tau - \tau') \cdot \mathbf{A}^{-1}]_{NN} \Big|_0^\tau \\ &\quad - \frac{1}{\omega} \int_0^\tau d\tau' [\sin(\omega\tau') (\mathbf{D} \cdot \mathbf{A}) \cdot \mathbf{G}(\tau - \tau') \cdot \mathbf{A}^{-1}]_{NN} \end{aligned} \quad (56)$$

Processing the second integral on the RHS of the above equation by parts,

$$\begin{aligned} \int_0^\tau d\tau' [\sin(\omega\tau') (\mathbf{D} \cdot \mathbf{A}) \cdot \mathbf{G}(\tau - \tau') \cdot \mathbf{A}^{-1}]_{NN} &= -\frac{1}{\omega} [\cos(\omega\tau') (\mathbf{D} \cdot \mathbf{A}) \cdot \mathbf{G}(\tau - \tau') \cdot \mathbf{A}^{-1}]_{NN} \Big|_0^\tau \\ &\quad + \frac{1}{\omega} \int_0^\tau d\tau' [\cos(\omega\tau') (\mathbf{D} \cdot \mathbf{A})^2 \cdot \mathbf{G}(\tau - \tau') \cdot \mathbf{A}^{-1}]_{NN} \end{aligned} \quad (57)$$

Plugging eq. (57) into eq. (56) and simplifying,

$$\begin{aligned} &\int_0^\tau d\tau' [\cos(\omega\tau') \{ \omega^2 \boldsymbol{\delta} + (\mathbf{D} \cdot \mathbf{A})^2 \} \cdot \mathbf{G}(\tau - \tau') \cdot \mathbf{A}^{-1}]_{NN} \\ &= [\omega \sin(\omega\tau) \mathbf{A}^{-1}]_{NN} \\ &\quad + [\cos(\omega\tau') (\mathbf{D} \cdot \mathbf{A}) \cdot \mathbf{G}(\tau - \tau') \cdot \mathbf{A}^{-1}]_{NN} \Big|_0^\tau \end{aligned} \quad (58)$$

The above equality holds for not just the $(NN)^{\text{th}}$ matrix element, but also for the matrices themselves. Therefore, we may write

$$\begin{aligned} &\int_0^\tau d\tau' [\cos(\omega\tau') \{ \omega^2 \boldsymbol{\delta} + (\mathbf{D} \cdot \mathbf{A})^2 \} \cdot \mathbf{G}(\tau - \tau') \cdot \mathbf{A}^{-1}] \\ &= [\omega \sin(\omega\tau) \mathbf{A}^{-1}] \\ &\quad + [\cos(\omega\tau') \mathbf{G}(\tau - \tau') \cdot (\mathbf{D} \cdot \mathbf{A}) \cdot \mathbf{A}^{-1}] \Big|_0^\tau \end{aligned} \quad (59)$$

Defining

$$\boldsymbol{\Phi} = [\omega^2 \boldsymbol{\delta} + (\mathbf{D} \cdot \mathbf{A})^2]^{-1} \quad (60)$$

and premultiplying by $\boldsymbol{\Phi}$ on both sides of eq. (59), yields, after simplification,

$$\begin{aligned} &\int_0^\tau d\tau' [\cos(\omega\tau') \mathbf{G}(\tau - \tau') \cdot \mathbf{A}^{-1}] = [\omega \sin(\omega\tau) \boldsymbol{\Phi} \cdot \mathbf{A}^{-1} \\ &\quad + \cos(\omega\tau) \boldsymbol{\Phi} \cdot \mathbf{D} - \boldsymbol{\Phi} \cdot \mathbf{G}(\tau) \cdot \mathbf{D}] \end{aligned} \quad (61)$$

Since the above matrix relation also holds true for the $(NN)^{\text{th}}$ element, we therefore have

$$\begin{aligned} \int_0^\tau d\tau' [\cos(\omega\tau') \mathbf{G}(\tau - \tau') \cdot \mathbf{A}^{-1}]_{NN} &= [\omega \sin(\omega\tau) \boldsymbol{\Phi} \cdot \mathbf{A}^{-1} \\ &\quad + \cos(\omega\tau) \boldsymbol{\Phi} \cdot \mathbf{D} - \boldsymbol{\Phi} \cdot \mathbf{G}(\tau) \cdot \mathbf{D}]_{NN} \end{aligned} \quad (62)$$

Substituting eq. (62) into eq. (55), we obtain

$$\begin{aligned} \langle W_{\text{dis}} \rangle &= c^2 d^2 \omega^2 \int_0^{\tau_m} d\tau [\omega \cos(\omega\tau) \sin(\omega\tau) \boldsymbol{\Phi} \cdot \mathbf{A}^{-1}]_{NN} \\ &\quad + c^2 d^2 \omega^2 \int_0^{\tau_m} d\tau [\cos^2(\omega\tau) \boldsymbol{\Phi} \cdot \mathbf{D}]_{NN} \\ &\quad - c^2 d^2 \omega^2 \int_0^{\tau_m} d\tau [\cos(\omega\tau) \boldsymbol{\Phi} \cdot \mathbf{G}(\tau) \cdot \mathbf{D}]_{NN} \end{aligned} \quad (63)$$

The first two integrals on the RHS of the above equation are easily evaluated, using the double-angle formulae $\cos(\omega\tau) \sin(\omega\tau) = (1/2)[\sin(2\omega\tau)]$ and $\cos^2(\omega\tau) = (1/2)[1 + \cos(2\omega\tau)]$, respectively, to give

$$\int_0^{\tau_m} d\tau [\omega \cos(\omega\tau) \sin(\omega\tau) \Phi \cdot \mathbf{A}^{-1}]_{NN} = \frac{1}{4} [1 - \cos(2\omega\tau_m)] [\Phi \cdot \mathbf{A}^{-1}]_{NN} \quad (64)$$

$$\int_0^{\tau_m} d\tau [\cos^2(\omega\tau) \Phi \cdot \mathbf{D}]_{NN} = \left[\frac{\tau_m}{2} + \frac{\sin(2\omega\tau_m)}{4\omega} \right] [\Phi \cdot \mathbf{D}]_{NN} \quad (65)$$

The last integral on the RHS of eq. (63) is evaluated by parts, as follows

$$\begin{aligned} \int_0^{\tau_m} d\tau [\cos(\omega\tau) \Phi \cdot \mathbf{G}(\tau) \cdot \mathbf{D}]_{NN} &= \frac{1}{\omega} [\sin(\omega\tau) \Phi \cdot \mathbf{G}(\tau) \cdot \mathbf{D}]_{NN} \Big|_0^{\tau_m} \\ &- \frac{1}{\omega} \int_0^{\tau_m} d\tau [\sin(\omega\tau) \Phi \cdot (\mathbf{D} \cdot \mathbf{A}) \cdot \mathbf{G}(\tau) \cdot \mathbf{D}]_{NN} \end{aligned} \quad (66)$$

Processing the second integral on the RHS of the above equation by parts, and simplifying eq. (66) using a procedure identical to that adopted in eqs. (58)-(62), we get

$$\begin{aligned} \int_0^{\tau_m} d\tau [\cos(\omega\tau) \Phi \cdot \mathbf{G}(\tau) \cdot \mathbf{D}]_{NN} &= \\ &\left[\omega \sin(\omega\tau_m) \Phi^2 \cdot \mathbf{G}(\tau_m) \cdot \mathbf{D} \right. \\ &\left. + \cos(\omega\tau_m) \Phi^2 \cdot (\mathbf{D} \cdot \mathbf{A}) \cdot \mathbf{G}(\tau_m) \cdot \mathbf{D} - \Phi^2 \cdot \mathbf{D} \cdot \mathbf{A} \cdot \mathbf{D} \right]_{NN} \end{aligned} \quad (67)$$

Substituting eqs. (64), (65), and (67) into eq. (63) and simplifying, we obtain

$$\begin{aligned} \langle W_{\text{dis}} \rangle &= \frac{c^2 d^2 \omega^2}{4} [1 - \cos(2\omega\tau_m)] [\Phi \cdot \mathbf{A}^{-1}]_{NN} \\ &+ \frac{c^2 d^2 \omega}{4} [2\omega\tau_m + \sin(2\omega\tau_m)] [\Phi \cdot \mathbf{D}]_{NN} \\ &- c^2 d^2 \omega^3 [\sin(\omega\tau_m) \Phi^2 \cdot \mathbf{G}(\tau_m) \cdot \mathbf{D}]_{NN} \\ &+ c^2 d^2 \omega^2 [\cos(\omega\tau_m) \Phi^2 \cdot (\mathbf{D} \cdot \mathbf{A}) \cdot \mathbf{G}(\tau_m) \cdot \mathbf{D}]_{NN} \\ &- c^2 d^2 \omega^2 [\Phi^2 \cdot \mathbf{D} \cdot \mathbf{A} \cdot \mathbf{D}]_{NN} \end{aligned} \quad (68)$$

We have required for the current protocol that $\omega\tau_m = \pi/2$, as illustrated in eq. (53). With this simplification, eq. (68) becomes

$$\begin{aligned} \langle W_{\text{dis}} \rangle &= \frac{c^2 d^2 \omega^2}{2} [\Phi \cdot \mathbf{A}^{-1}]_{NN} + \frac{c^2 d^2 \omega \pi}{4} [\Phi \cdot \mathbf{D}]_{NN} \\ &- c^2 d^2 \omega^3 [\Phi^2 \cdot \mathbf{G}(\tau_m) \cdot \mathbf{D}]_{NN} \\ &- c^2 d^2 \omega^2 [\Phi^2 \cdot \mathbf{D} \cdot \mathbf{A} \cdot \mathbf{D}]_{NN} \end{aligned} \quad (69)$$

IV. COMPARISON AGAINST PRIOR RESULTS

We now compare eq. (51) against results for two special cases which are available in the literature. Dhar⁴³ derived an expression for the variance of the work fluctuations for a Rouse chain without internal friction ($K = 0$) subjected to constant velocity pulling, with the steering spring of the same stiffness as the springs in the chain ($c = 1$).

Setting $K = 0$ in eq. (8) and $c = 1$ in eq. (51), we obtain $\mathbf{D} = \boldsymbol{\delta}$, and

$$\sigma_{\text{Rouse}}^2 = \frac{2d^2}{\tau_m} \left\{ \mathbf{A}^{-2} + \frac{1}{\tau_m} \mathbf{A}^{-3} \cdot [\exp[-\mathbf{A}\tau_m] - \boldsymbol{\delta}] \right\}_{NN}$$

which corresponds identically to eq. (19) in ref. 43, where the author has used the notation a (instead of d as done in the present work) to denote the pulling distance.

The work-statistics for a single-mode bead-spring-dashpot subjected to constant velocity pulling was derived in ref. 33, in which the stiffness of the steering spring was taken to be c_2 . Setting $N = 1$ and $c = c_2$, we obtain,

$$\begin{aligned} [\mathbf{A}]_{NN} &= (c_2 + 1) \\ [\mathbf{L}]_{NN} &= 1 \\ [\mathbf{D}]_{NN} &= \left[1 + \left(\frac{K}{\zeta} \right) \right]^{-1} = \left[\frac{\zeta}{\zeta + K} \right] \end{aligned} \quad (70)$$

and the dimensionless work

$$\begin{aligned} \langle W_{\text{dis}} \rangle_{N=1} &= \frac{(\zeta + K)}{\zeta} \left(\frac{c_2}{c_2 + 1} \right)^2 v d \\ &+ \frac{c_2^2}{(c_2 + 1)^3} \left(\frac{\zeta + K}{\zeta} \right)^2 \left[\exp \left(-\frac{\zeta (c_2 + 1) \tau_m}{(\zeta + K)} \right) - 1 \right] v^2 \end{aligned}$$

Denoting the dimensional variables with an asterisk, we have $d = d^* \sqrt{H/k_B T}$, $\tau_m = H t_m^* / \zeta$ and $v =$

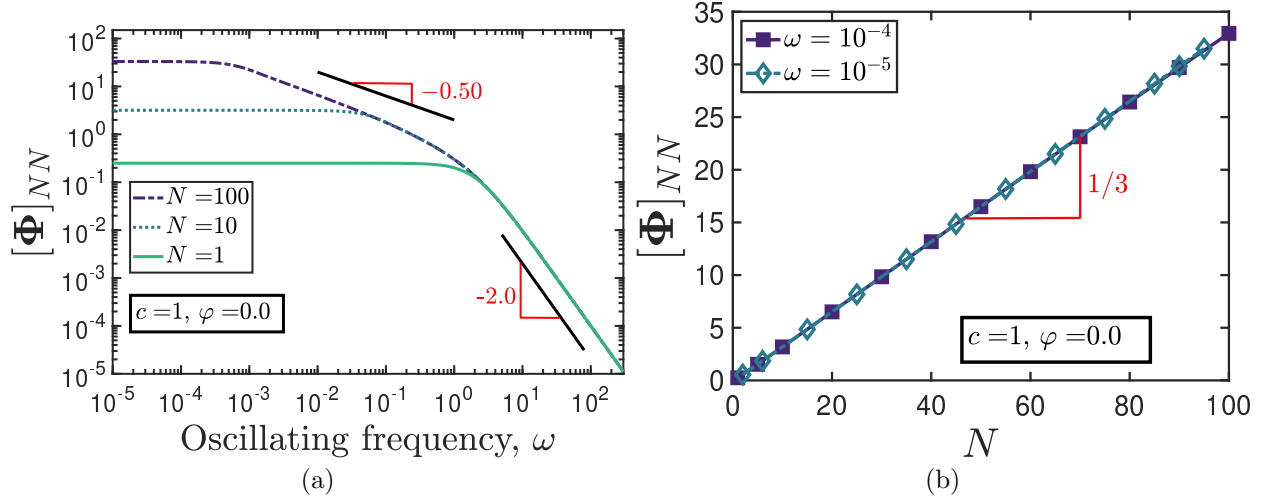


FIG. 2. The $(NN)^{\text{th}}$ term of the Φ matrix for a Rouse chain ($\varphi = 0$) pulled over a distance $d = 1$ using a steering spring of stiffness $c = 1$ as function of (a) driving frequency and (b) chain length. The values in (b) are evaluated for discrete values of N , and the line is a guide to the eye.

$v^* \zeta / \sqrt{k_B T H}$, we obtain

$$\begin{aligned} \langle W_{\text{dis}}^* \rangle_{N=1} &= \left(\frac{c_2}{c_2 + 1} \right)^2 (\zeta + K) v^* d^* \\ &+ \frac{c_2^2}{(c_2 + 1)^3} \frac{(\zeta + K)^2 v^{*2}}{H} \left[\exp \left(-\frac{H (c_2 + 1) d^*}{(\zeta + K) v^*} \right) - 1 \right], \end{aligned} \quad (71)$$

which agrees identically with eq. (16) in ref. 33. We report the value of the dimensionless dissipation for a dumbbell in the limit of large trap stiffness here:

$$\lim_{c \rightarrow \infty} \langle W_{\text{dis}} \rangle_{N=1} = (1 + \varphi) v d \quad (72)$$

as it will be useful for later discussion in the manuscript.

Speck and Seifert⁴⁴ have studied Rouse chains (without internal friction) subjected to constant velocity pulling and oscillatory driving. In their paper, the last bead of the Rouse chain is directly manipulated to move at a prescribed velocity (or frequency) and is not attached to a steering spring. Their results may be extended to describe the case of a chain being pulled by a steering spring with a different stiffness, but the paper⁴⁴ only reports results for the case where all the springs are of the same stiffness. To compare our results with theirs, we set $c = 1$, and note for a Rouse chain that

$$\begin{aligned} D &= D^{-1} = \delta \\ \Phi &= [\omega^2 \delta + A^2]^{-1} \end{aligned} \quad (73)$$

resulting in the following expression for the dissipation

$$\begin{aligned} \langle W_{\text{dis}} \rangle_{\text{Rouse}} &= \frac{d^2 \omega^2}{4} [1 - \cos(2\omega \tau_m)] [\Phi \cdot A^{-1}]_{NN} \\ &+ \frac{d^2 \omega}{4} [2\omega \tau_m + \sin(2\omega \tau_m)] [\Phi]_{NN} \\ &- d^2 \omega^3 [\sin(\omega \tau_m) \Phi^2 \cdot G(\tau_m)]_{NN} \\ &+ d^2 \omega^2 [\cos(\omega \tau_m) \Phi^2 \cdot A \cdot G(\tau_m)]_{NN} - d^2 \omega^2 [\Phi^2 \cdot A]_{NN} \end{aligned} \quad (74)$$

We next seek to obtain an expression for the dissipation in the limit of slow driving ($\omega \ll 1$). In the absence of an analytical expression for Φ , we numerically evaluate the $(NN)^{\text{th}}$ element of this matrix and plots its dependence on frequency and chain length in Fig. 2.

We observe that Φ_{NN} has a low frequency plateau whose value varies linearly with the chain length. In the slow driving regime, therefore, we may only retain terms from eq. (74) that are linear in ω , and reject the higher-order terms, to give

$$\begin{aligned} \lim_{\omega \ll 1} \langle W_{\text{dis}} \rangle_{\text{Rouse}} &\approx \frac{d^2 \omega}{4} [2\omega \tau_m + \sin(2\omega \tau_m)] [\Phi]_{NN} \\ &= \frac{N d^2 \omega}{3} \frac{1}{4} [2\omega \tau_m + \sin(2\omega \tau_m)] \end{aligned} \quad (75)$$

where the equality in the second line follows from Fig. 2 (b), by replacing the $(NN)^{\text{th}}$ element of Φ with $(N/3)$ in the limit of slow driving. Using $d = d^* \sqrt{H/k_B T}$, $\tau_m = H t_m^* / \zeta$ and $\omega = \omega^* \zeta / H$ to cast

eq. (75) in its dimensional form,

$$\langle W_{\text{dis}}^* \rangle_{\text{Rouse}} = \frac{N\zeta}{3} \frac{d^{2*}\omega^*}{4} [2\omega^*\tau_m^* + \sin(2\omega^*\tau_m^*)] \quad (76)$$

We reproduce below eq. (66) exactly as it appears in the paper by Speck and Seifert⁴⁴, which is an analytical expression for the average dimensional dissipation in the slow driving regime:

$$\overline{W_d} = \frac{N\gamma}{3} \frac{L^2\omega}{4} [2\omega t_s + \sin(2\omega t_s)] \quad (77)$$

where γ is the friction coefficient, which is denoted by ζ

in this manuscript. The term L represents the distance over which the last bead is moved over a time interval t_s , whose equivalents are d^* and τ_m^* in the present work. The excellent agreement between eqs. (76) and (77) provide a validation of the work expression derived in this manuscript.

It is also instructive to write the expression for dissipation incurred in subjecting a single-mode spring-dashpot ($N = 1$) to oscillatory driving, as this result will be discussed later in the manuscript. For $N = 1$, eq. (70) applies, along with

$$\begin{aligned} [\Phi]_{NN} &= \frac{(1+\varphi)^2}{\omega^2(1+\varphi)^2 + (c+1)^2} \\ [\Phi \cdot \mathbf{A}^{-1}]_{NN} &= \left(\frac{1}{c+1} \right) \left[\frac{(1+\varphi)^2}{\omega^2(1+\varphi)^2 + (c+1)^2} \right] \\ [\Phi \cdot \mathbf{D}]_{NN} &= \left[\frac{(1+\varphi)}{\omega^2(1+\varphi)^2 + (c+1)^2} \right] \\ [\Phi^2 \cdot \mathbf{G}(\tau_m) \cdot \mathbf{D}]_{NN} &= \frac{(1+\varphi)^3}{[\omega^2(1+\varphi)^2 + (c+1)^2]^2} \exp \left[-\frac{c+1}{1+\varphi} \tau_m \right] \\ [\Phi^2 \cdot (\mathbf{D} \cdot \mathbf{A}) \cdot \mathbf{G}(\tau_m) \cdot \mathbf{D}]_{NN} &= \frac{(1+\varphi)^2(c+1)}{[\omega^2(1+\varphi)^2 + (c+1)^2]^2} \exp \left[-\frac{c+1}{1+\varphi} \tau_m \right] \\ [\Phi \cdot \mathbf{D} \cdot \mathbf{A} \cdot \mathbf{D}]_{NN} &= \frac{(1+\varphi)^2(c+1)}{[\omega^2(1+\varphi)^2 + (c+1)^2]^2} \end{aligned} \quad (78)$$

Substituting eq. (78) into eq. (69) and simplifying,

$$\begin{aligned} \langle W_{\text{dis}} \rangle_{N=1} &= \frac{c^2 d^2 \omega^2}{2} \left(\frac{1}{c+1} \right) \left[\frac{(1+\varphi)^2}{\omega^2(1+\varphi)^2 + (c+1)^2} \right] + \frac{\pi c^2 d^2 \omega}{4} \left[\frac{(1+\varphi)}{\omega^2(1+\varphi)^2 + (c+1)^2} \right] \\ &\quad - \frac{c^2 d^2 \omega^3 (1+\varphi)^3}{[\omega^2(1+\varphi)^2 + (c+1)^2]^2} \exp \left[-\frac{c+1}{1+\varphi} \tau_m \right] - \frac{c^2 d^2 \omega^2 (1+\varphi)^2 (c+1)}{[\omega^2(1+\varphi)^2 + (c+1)^2]^2} \end{aligned} \quad (79)$$

In the limit of large steering spring stiffness ($c \rightarrow \infty$), we recognize that eq. (79) becomes

$$\lim_{c \rightarrow \infty} \langle W_{\text{dis}} \rangle_{N=1} = \frac{\pi d^2 \omega}{4} (1+\varphi) \quad (80)$$

while taking the limit of a large driving frequency ($\omega \rightarrow$

∞) in eq. (79) results in

$$\lim_{\omega \rightarrow \infty} \langle W_{\text{dis}} \rangle_{N=1} = \frac{d^2}{2} \frac{c^2}{c+1} + \frac{c^2 d^2 \pi}{4(1+\varphi)} \quad (81)$$

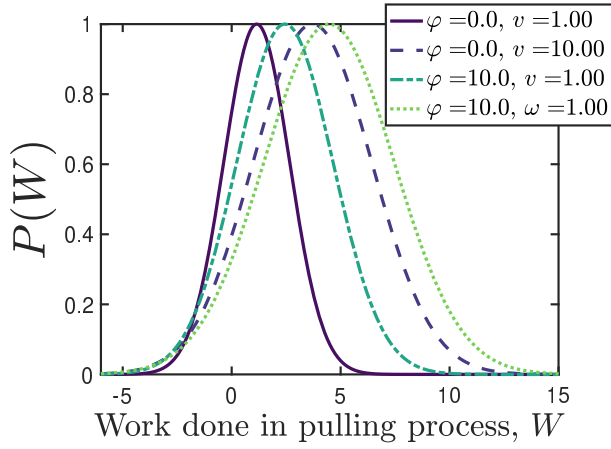


FIG. 3. Probability distribution of work for a chain with $N = 100$ subjected to various pulling protocols over a distance of $d = 1$, using a steering spring of stiffness $c = 10$. The beginning position of the trap is set to the origin for all the cases, i.e., $\alpha(0) = 0$.

V. RESULTS AND DISCUSSION

The probability distribution of work done, $P(W)$, is a Gaussian whose expression is given by

$$P(W) = \frac{1}{\sqrt{2\pi\sigma^2}} e^{-(W-\langle W \rangle)^2/2\sigma^2} \quad (82)$$

which implies that the Jarzynski equality, $\langle \exp[-W/k_B T] \rangle = \exp[-\Delta F/k_B T]$, is trivially satisfied for this system^{33,47,53}.

The mean of the Gaussian is given by eq. (33), where the free energy difference in transitioning between the initial state (at $\tau = 0$) and the final state ($\tau = \tau_m$) is the same for both the protocols considered in this manuscript, i.e.,

$$\begin{aligned} \Delta F &= F[\alpha(\tau_m)] - F[\alpha(0)] \\ &= \frac{cd}{2} [\alpha(\tau_m) + \alpha(0)] \{1 - c[\mathbf{A}^{-1}]_{NN}\} \end{aligned} \quad (83)$$

The dissipation for the two protocols, however, are different as evident from eq. (51) and eq. (69).

Fig. 3 illustrates the probability distribution given by eq. (82) for a variety of parameters. For a quasistatic process, the average work done in the pulling process is equal to the free energy change (by definition⁵⁴), and there is no associated dissipation. At finite rates of driving however, there is dissipation incurred even in the absence of internal friction, because the beads have to be pulled against the frictional resistance offered by the solvent. With the inclusion of internal friction, the dissipation (width of the distribution) increases for the same value of the pulling velocity. Higher the pulling velocity (or frequency), larger is the dissipation. A comparison between the dissipation incurred in the two protocols is provided

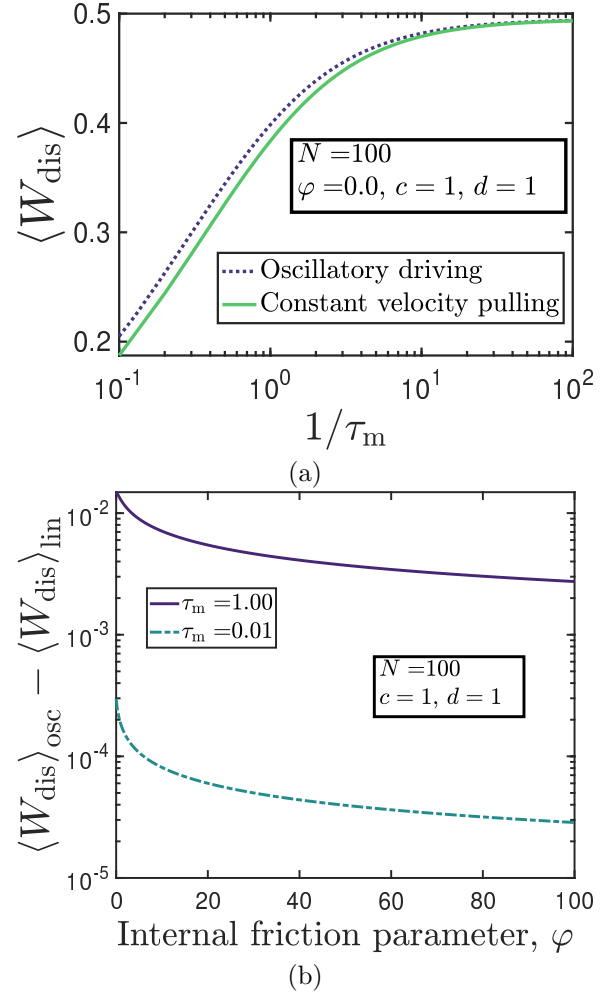


FIG. 4. (a) Average dissipated work as a function of protocol duration (τ_m) for a bead-spring-dashpot chain with $N = 100$ springs driven under the linear and symmetric protocols (b) Difference between the work dissipated in the two protocols as a function of the internal friction parameter, for the same value of the protocol duration.

by Fig. 4.

Fig. 4 (a) illustrates that for the same duration of the pulling protocol, τ_m , the work dissipated in oscillatory driving of a Rouse chain (without internal friction) is greater than that incurred in constant velocity pulling, in agreement with the findings of Speck and Seifert⁴⁴. The difference between the two protocols vanishes in the limit of slow pulling ($\tau_m \rightarrow 0$). Fig 4 (b) shows that the difference in dissipation due to the two protocols measured for the same protocol duration, decreases as a function of the internal friction parameter.

Constant velocity pulling (linear protocol)

The formal expression given by eq. 51, written entirely in terms of the matrix elements, does not provide an insight into the dependence of the dissipated work on factors such as the stiffness of the steering spring, the size of the polymer chain (N), or how the total dissipation

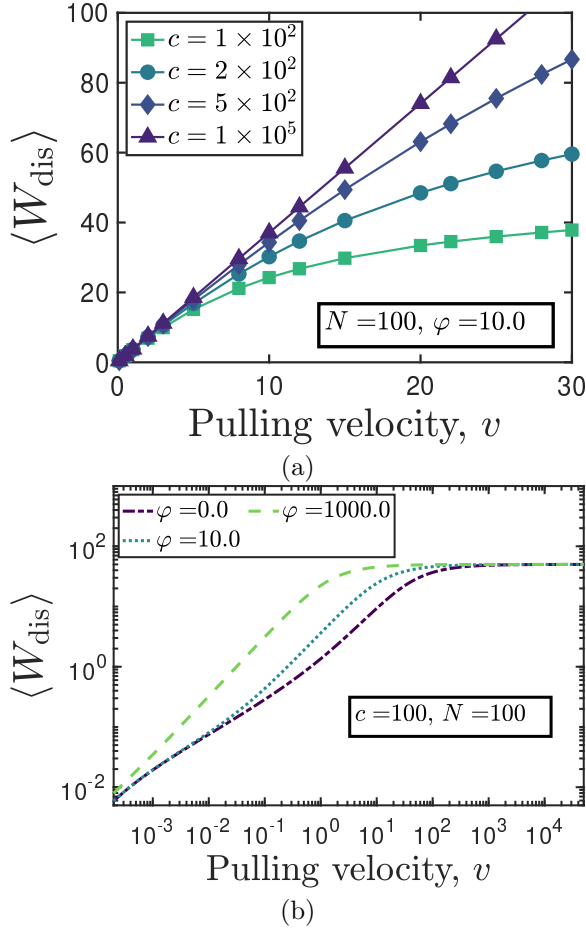


FIG. 5. Average dissipated work as a function of pulling velocity for a chain with internal friction, pulled over a constant dimensionless distance of $d = 1$, over (a) a moderate range of pulling velocities, at a fixed internal friction parameter ($\varphi = 10$) and various values of the steering spring stiffness, and (b) a larger range of pulling velocities, at a fixed steering spring stiffness ($c = 100$) and various values of the internal friction parameter.

relates to the damping coefficient of a single dashpot. We attempt to address these questions through numerical calculations.

Firstly, we note from Fig. 5 (a) that for a fixed chain size, pulling distance and dashpot damping coefficient, the dependence of dissipated work on the pulling velocity changes from being non-linear to linear with an increase in the stiffness of the steering spring. Additionally, Fig. 5 (b) illustrates that for a given value of the steering spring stiffness, the dissipated work attains a constant value in the limit of high pulling velocities. Increasing the internal friction parameter results in the attainment of the asymptotic dissipation value at smaller values of the pulling velocity.

The variation of dissipation as a function of the steering trap stiffness is shown in Fig. 6. For a fixed value of the chain length and the pulling distance, the dependence

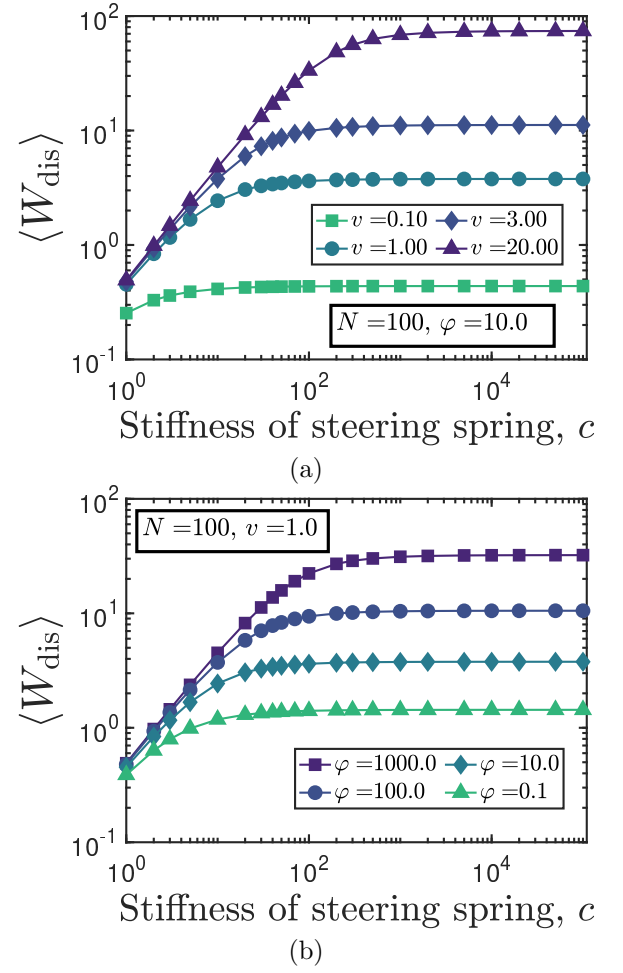


FIG. 6. Dissipated work as a function of the steering spring stiffness, for a bead-spring-dashpot chain (a) of fixed internal friction parameter ($\varphi = 10$) driven at various pulling velocities and (b) driven at a fixed pulling velocity ($v = 1.0$), possessing various values of the internal friction parameter.

of dissipation on the steering spring stiffness vanishes at large enough values of the latter, plateauing to a constant value. The spring stiffness at which the dissipation attains a constant value appears to be a function of both the pulling velocity and the internal friction coefficient. With an increase of either the internal friction coefficient or the pulling velocity, the plateau value of dissipation is reached at larger values of the steering spring stiffness.

A natural question to consider is how the dissipation varies as a function of the chain length? i.e., given a bead-spring-dashpot unit with a particular value of the spring stiffness and dashpot damping coefficient, how will the dissipation incurred in pulling such a setup change as more bead-spring-dashpots are added in series. The answer appears to be highly nontrivial, and dependent on the stiffness of the steering spring, as discussed below.

Fig. 7 illustrates the dissipated work as a function of the pulling velocity for bead-spring-dashpot chains of

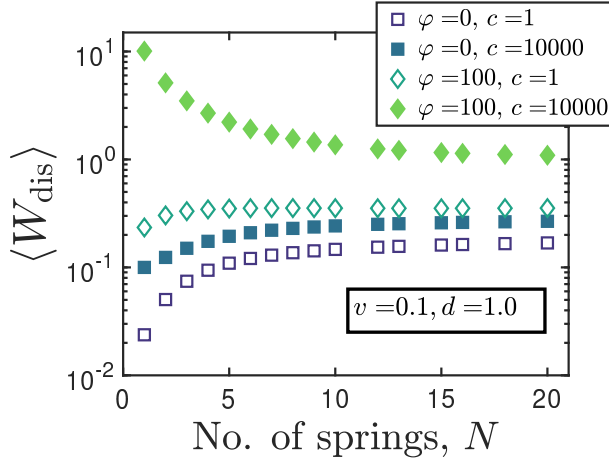


FIG. 7. Dissipated work as a function of chain length (N) at two values of the trap stiffness, measured for bead-spring-dashpot chains with and without internal friction, pulled at a constant velocity of $v = 0.1$ over a distance $d = 1.0$.

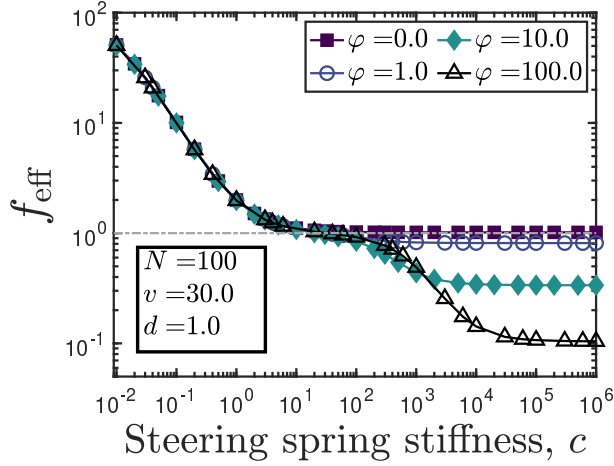


FIG. 8. Plot of f_{eff} [defined in eq. (84)] as a function of the steering spring stiffness, c , for a bead-spring-dashpot chain with $N = 100$, pulled at a velocity of $v = 30$ over a distance $d = 1$.

various lengths, for the case of a soft and stiff steering spring. In the absence of internal friction ($\varphi = 0$), the dissipation at each pulling velocity increases with chain length before ceasing to increase further, for both soft and stiff steering springs. The same trend is observed in the presence of internal friction, for bead-spring-dashpots pulled using a soft spring. This is straight forward, in that more work is dissipated in pulling a chain with two spring-dashpots, say, as compared to one with ten. We term this situation as being *cooperative*, as the spring-dashpots contribute additively towards the total dissipation. Note that the term additive is used in a loose sense because it is not known precisely if the contribution to the total dissipation from each spring-dashpot is exactly additive or some other function.

For chains with internal friction being pulled using a

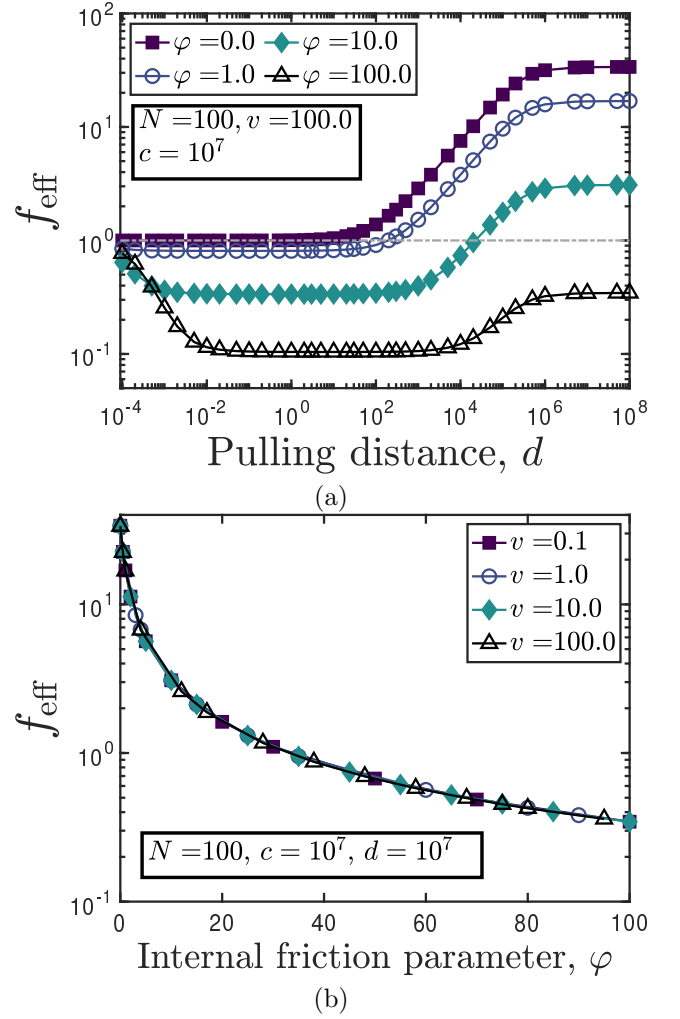


FIG. 9. Variation of f_{eff} [defined in eq. (84)] as a function of (a) pulling distance in the limit of high trap stiffness and (b) internal frictional parameter in the limit of large pulling distance and high trap stiffness, for a bead-spring-dashpot chain with $N = 100$ springs.

stiff steering spring, however, the dissipation incurred at each pulling velocity *decreases* with an increase in chain length. This appears surprising, because, it implies that pulling a chain with two spring-dashpot dissipates more work than one with ten spring-dashpots. We term this situation as being *anti-cooperative*, since the dissipation incurred by several dashpots is lower than a single spring-dashpot being pulled. This trend remains conserved even when the *total* work (not shown) and not just the dissipated work is considered. A transition from cooperative to anti-cooperative response is not observed in the absence of internal friction, however. We attempt to explain this seemingly counter-intuitive trend below, in the context of protein unfolding.

The force-induced unfolding of a protein molecule may be envisaged as a diffusive process over a rugged free-energy landscape^{22,55,56}, given the many competing

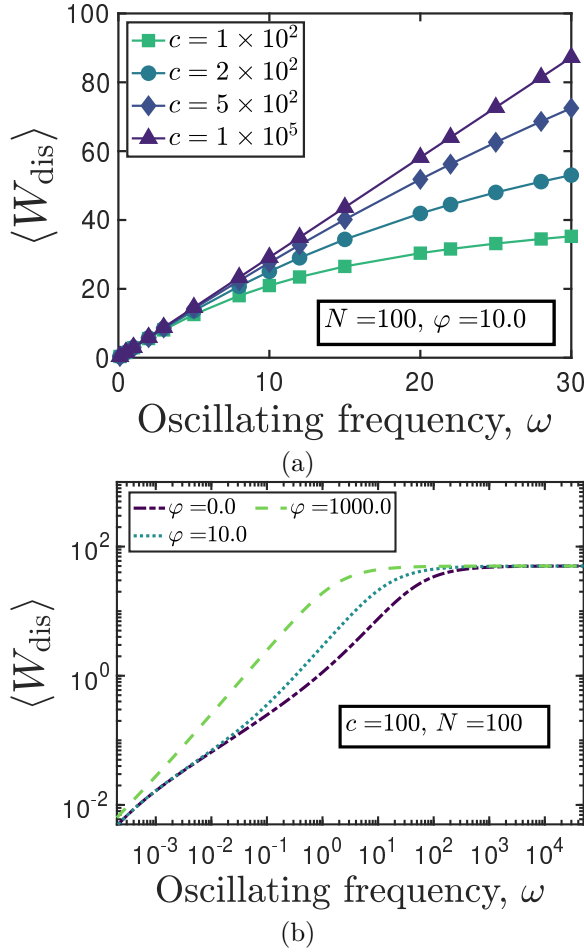


FIG. 10. Average dissipated work as a function of oscillating frequency for a chain with internal friction, pulled over a constant dimensionless distance of $d = 1$, over (a) a moderate range of driving frequencies, at a fixed internal friction parameter ($\varphi = 10$) and various values of the steering spring stiffness, and (b) a larger range of driving frequencies, at a fixed steering spring stiffness ($c = 100$) and various values of the internal friction parameter.

metastable states available for the molecule. In steered molecular dynamics (SMD) simulations^{57,58}, a harmonic trap is typically used to pull at one end of a tethered biomolecule, and the work statistics for the trajectory is recorded. The usual goal of these simulations is to extract the free energy profile of the molecule, i.e., how the free energy changes as a function of an internal reaction coordinate. Jarzynski's equality may be used to extract this information from the work trajectories provided that the reaction coordinate is well approximated by the position of the constraint (trap). The use of a stiff spring ensures that the reaction coordinate does not deviate too much from the constraint position, ensuring that the fluctuations in the trajectories are minimal and that the system does not explore highly dissipative pathways in a rugged energy landscape, resulting in a smaller

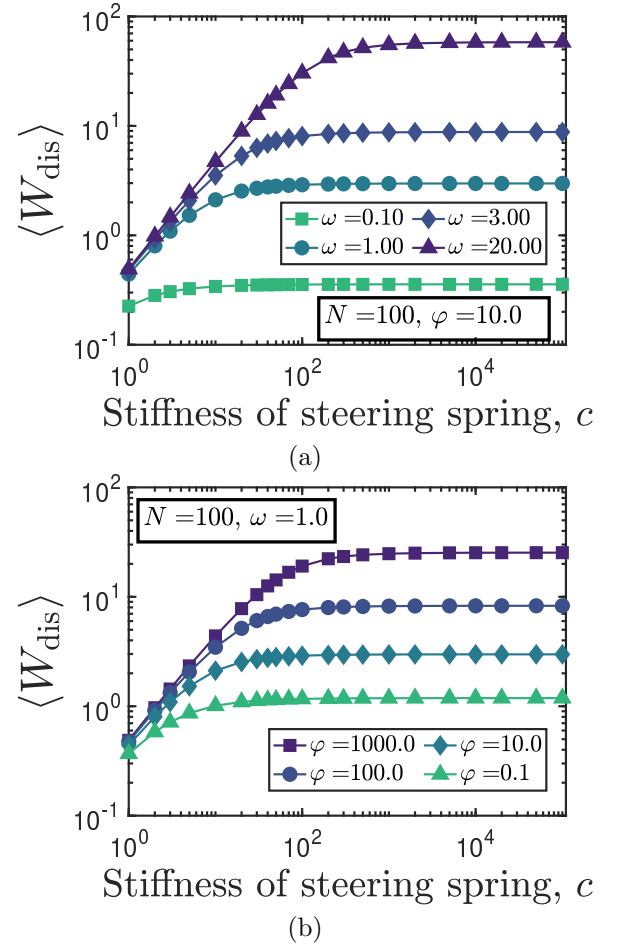


FIG. 11. Dissipated work as a function of the steering spring stiffness, for a bead-spring-dashpot chain (a) of fixed internal friction parameter ($\varphi = 10$) driven at various frequencies and (b) driven at a fixed frequency ($\omega = 1.0$), possessing various values of the internal friction parameter.

error of the computed free energy profile⁵⁹.

The usage of a harmonic trap with large stiffness to minimize the dissipation incurred in pulling a colloidal particle over an undulating energy landscape has also been reported by Sivak and coworkers^{60,61}. Specifically, they aim to develop a two-dimensional protocol for minimizing the dissipation associated with the above process, by tuning the position of the trap centre and the stiffness of harmonic confinement with time. They find that the protocol resulting minimal dissipation requires that the trap stiffness increase as the colloid crosses the barriers. Additionally, it is found that higher values of the initial trap stiffness result in lower values of the dissipation and hence higher efficiency.

The dissipative response of a series of spring-dashpots being pulled at a constant velocity is clearly dictated by the stiffness of the steering spring. We next examine the value of the spring-stiffness at which the dissipative response transitions from being cooperative to anti-

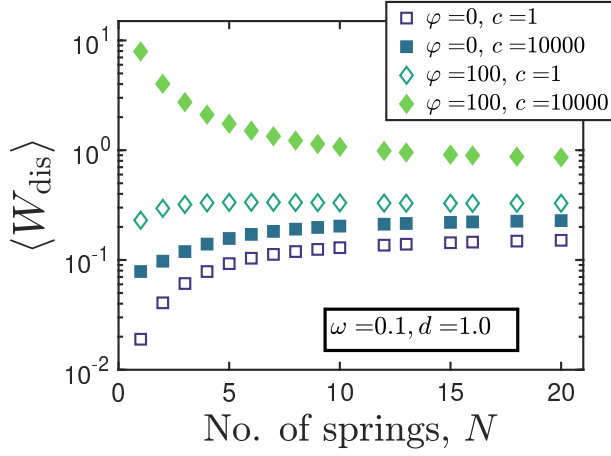


FIG. 12. Dissipated work as a function of chain length (N) at two values of the trap stiffness, measured for bead-spring-dashpot chains with and without internal friction, driven at a constant frequency of $\omega = 0.1$ over a distance $d = 1.0$.

cooperative, and its dependence on the internal friction coefficient. We introduce the quantity $f_{\text{eff}}(N; \varphi, v, c, d)$ which is a ratio of the work dissipated by a chain of N bead-spring-dashpots to a single bead-spring-dashpot, at fixed values of the pulling velocity, pulling distance, the dashpot damping coefficient and the steering spring stiffness.

$$f_{\text{eff}}(N; \varphi, v, c, d) = \frac{\langle W_{\text{dis}} \rangle_N}{\langle W_{\text{dis}} \rangle_{N=1}} \bigg|_{\varphi, v, c, d} \quad (84)$$

A value of $f_{\text{eff}} > 1$ suggests cooperative behavior, while $f_{\text{eff}} < 1$ is indicative of an anticooperative response. A two-bead spring subjected to pulling will therefore have a value of $f_{\text{eff}} = 1$ by definition, at all values of the steering spring stiffness. In the limit of large pulling spring stiffness, the following relationship can be written between the work dissipated in a bead-spring-dashpot chain with N spring-dashpots to that dissipated by a single spring-dashpot (cf. eq. (72)):

$$\lim_{c \rightarrow \infty} \langle W_{\text{dis}} \rangle_N = f_{\text{eff}}(1 + \varphi)vd \quad (85)$$

Fig. 8 illustrates the variation of f_{eff} as a function of the steering spring stiffness for various values of the internal friction coefficient. We observe that the steering spring stiffness at which the transition from cooperative to anticooperative response occurs is a function of the pulling velocity and distance. In the limit of large trap stiffness, f_{eff} attains a plateau that is dependent on the internal friction parameter, at constant values of the pulling velocity and distance.

Fig. 9 (a) illustrates the variation of f_{eff} as a function of the pulling distance, in the limit of large steering spring stiffness, for chains with various values of the internal friction parameter. At infinitesimally small values

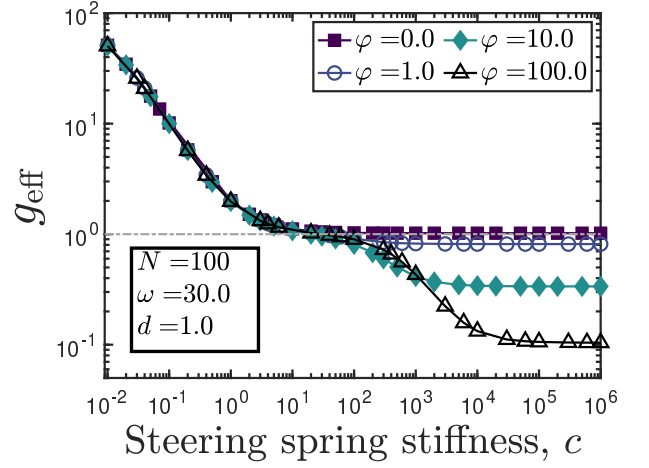


FIG. 13. Plot of g_{eff} [defined in eq. (86)] as a function of the steering spring stiffness, for a bead-spring-dashpot chain with $N = 100$, driven at a frequency of $\omega = 30$ over a distance $d = 1$.

of the pulling distance, the value of f_{eff} is unity for all values of the internal friction parameter. In the limit of large pulling distance, f_{eff} attains a plateau value that is dependent on the internal friction parameter. For large values of the pulling distance and trap stiffness, Fig. 9 (b) illustrates that f_{eff} is independent of the pulling velocity, and is only a function of the internal friction parameter.

Owing to this dependence of f_{eff} on the internal friction coefficient, it cannot be estimated *a priori*. This is in direct contrast with the single mode spring-dashpot, for which $f_{\text{eff}} = 1$ irrespective of the internal friction coefficient. Consequently, it is not possible in general to establish a relationship between the total dissipation in pulling a bead-spring-dashpot chain at constant velocity and the damping coefficient of a single dashpot. The specific case of a single-mode spring dashpot is an exception, and is relatively easier to analyze, as discussed in ref. 6.

Oscillatory driving (symmetric protocol)

The variation of the dissipation incurred in oscillatory driving as a function of frequency shows a near-identical trend to that observed in constant velocity pulling. As illustrated in Fig. 10 (a), over a moderate range of driving frequencies, the scaling of dissipation with respect to the frequency goes from being non-linear to linear as the trap stiffness is increased, keeping all other parameters fixed. Furthermore, Fig. 10 (b) shows that the dissipation incurred in the large frequency limit is a function of the trap stiffness and is independent of the internal friction parameter. The inclusion of internal friction results in the attainment of the asymptotic dissipation value at lower frequencies.

Fig. 11 illustrates that the dissipated work increases with the steering trap stiffness, before attaining a constant value that depends on the frequency of the driving and the internal friction parameter. This trend is identical to that observed for the case of constant velocity pulling.

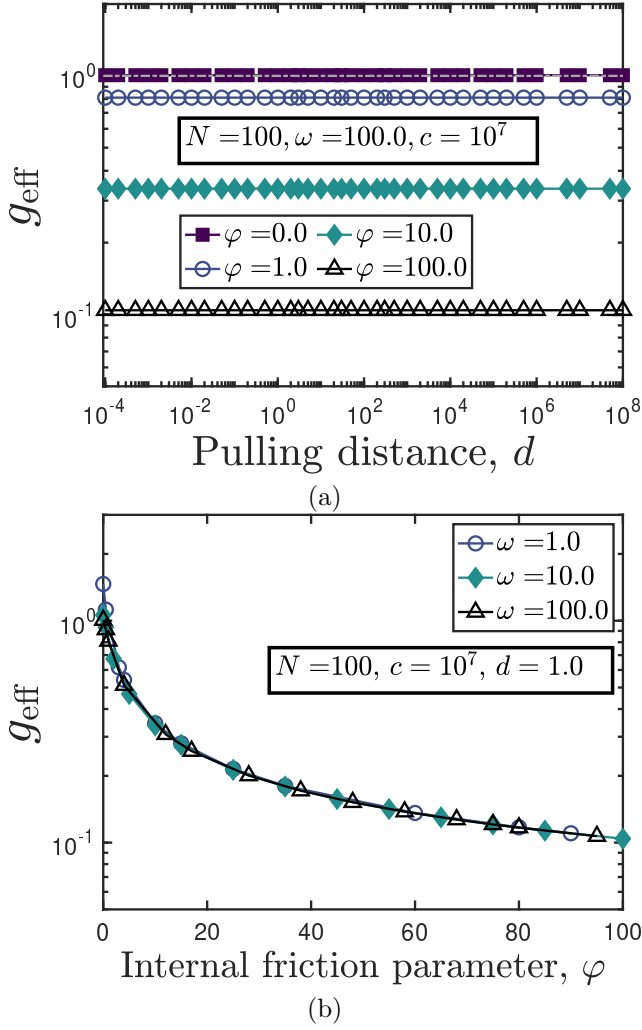


FIG. 14. Variation of g_{eff} [defined in eq. (86)] as a function of (a) pulling distance and (b) internal frictional parameter in the limit of high trap stiffness for a bead-spring-dashpot chain with $N = 100$ springs.

In addressing the question of how the dissipation in oscillatory driving scales with the chain length, we encounter a similar trend as observed for the case of constant velocity pulling. As seen from Fig. 12, for chains without internal friction, the dissipation increases with the number of springs in the chain, irrespective of the stiffness of the steering spring, and saturates to a constant value. With the inclusion of internal friction, however, the steering spring stiffness determines if the dissipation increases or decreases with the number of spring-dashpots in the chain.

The transition from cooperative to anti-cooperative response is observed in the case of oscillatory driving as well, and we introduce the metric $g_{\text{eff}}(N; \varphi, \omega, c, d)$ to quantify this phenomenon, which is defined as the ratio of work done dissipated in driving a N -spring-dashpot chain with internal friction parameter φ over a distance

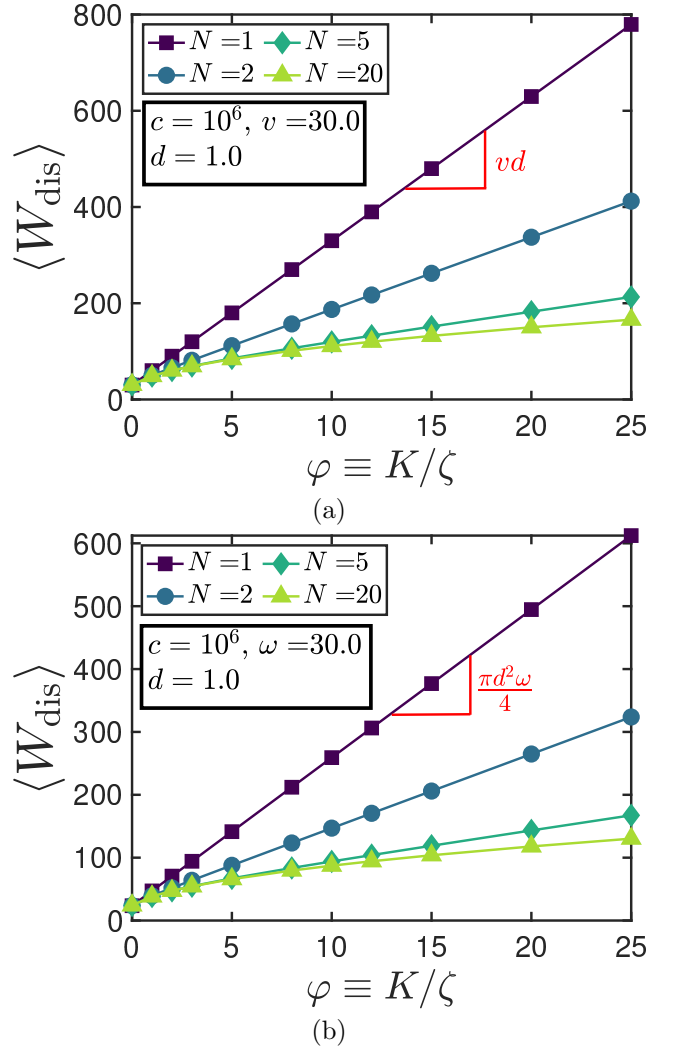


FIG. 15. Variation of dissipated work as a function of the internal friction parameter for (a) constant velocity pulling (linear protocol) and (b) oscillatory driving (symmetric) protocol, for chains of various lengths. The pulling trap stiffness and pulling distance are fixed at $c = 10^6$ and $d = 1$ for both the cases.

d at a frequency ω , to that dissipated in driving a single spring-dashpot ($N = 1$) at the same set of parameter values. Mathematically,

$$g_{\text{eff}}(N; \varphi, \omega, c, d) = \frac{\langle W_{\text{dis}} \rangle_N}{\langle W_{\text{dis}} \rangle_{N=1}} \bigg|_{\varphi, \omega, c, d} \quad (86)$$

A value of $g_{\text{eff}} > 1$ suggests cooperative behavior, while $g_{\text{eff}} < 1$ is indicative of an anticooperative response. A two-bead spring subjected to oscillatory driving will therefore have a value of $g_{\text{eff}} = 1$ by definition, at all values of the steering spring stiffness. In the limit of large pulling spring stiffness, the following relationship may be written between the work dissipated in a bead-spring-

dashpot chain with N spring-dashpots to that dissipated by a single spring-dashpot (cf. eq. (80)):

$$\lim_{c \rightarrow \infty} \langle W_{\text{dis}} \rangle_N = g_{\text{eff}} \left[\frac{\pi d^2 \omega}{4} (1 + \varphi) \right] \quad (87)$$

Fig. 13 shows the variation of g_{eff} as a function of the steering spring stiffness for bead-spring-dashpot chains with various internal friction parameter values, for fixed values of chain length, pulling distance and driving frequency. The crossover from cooperative ($g_{\text{eff}} > 1$) to anti-cooperative response ($g_{\text{eff}} < 1$) is observed only in the presence of internal friction, i.e., $\varphi > 0$, similar to that observed in constant velocity pulling.

In a major departure from the constant velocity pulling case, however, g_{eff} is not a function of the pulling distance, as evinced in Fig. 14 (a). The limiting value of g_{eff} at high spring stiffness is then observed to be a function of the internal friction parameter alone, and is independent of the driving frequency, as illustrated in Fig. 14 (b).

The dependence of the prefactor g_{eff} (f_{eff}) on the internal friction parameter in the symmetric (linear) protocol therefore implies that the work dissipated in the process does not scale linearly with the internal friction parameter in the limit of high trap stiffness.

Fig. 15 illustrates the scaling of the dissipated work as a function of the internal friction parameter for various values of the chain length. In the limit of high trap stiffness, for both the driving protocols considered in this manuscript, the dissipation goes from being a linear function of φ for the $N = 1$ case, to a sub-linear function of φ as the value of N is increased.

VI. OUTLOOK AND CONCLUSIONS

We have numerically evaluated the work statistics for a coarse-grained polymer model with internal friction subjected to driving protocols commonly encountered in single-molecule force spectroscopy experiments, namely, constant velocity (linear) and oscillatory (symmetric) pulling. The use of Hookean springs results in the work distribution being Gaussian and Jarzynski's equality is satisfied for the system and protocols discussed in the present work. The dependence of the dissipated work with the pulling trap stiffness, the internal friction parameter and the length of the chain are assessed for both the protocols.

While the connection between the dissipation incurred in pulling a bead-spring-dashpot chain and the damping coefficient of the dashpot is readily apparent for the case

of a dumbbell ($N = 1$), it is difficult to establish such a relation for chains with $N > 1$. In the limit of high trap stiffness, we have formally shown that $\langle W_{\text{dis}} \rangle \propto \varphi$, where the prefactors are simply the pulling velocity and distance, and independent of the internal friction parameter. For chains with $N > 1$, the relationship is no-longer straightforward, since the dissipation depends on a prefactor that is a function of the internal friction parameter, and which cannot be ascertained *a priori*. It is worth investigating if a transition between nonequilibrium steady states, where the strength of the flowfield experienced by the polymer chain is varied according to a set protocol^{62–68}, may illuminate the connection between the work dissipated in stretching the chain and the damping coefficient of an individual dashpot.

Additionally, the dissipation of chains in the high trap stiffness limit is found to scale inversely with the number of spring-dashpots in the chain, a phenomenon that we attempt to explain by analogy with a colloid being pulled over an undulating energy landscape using a harmonic trap. Conformational transitions in a protein molecule have routinely been compared to diffusion over a rugged energy landscape^{22,56}, and related to the internal friction of the molecule¹⁴. A larger number of bead-spring-dashpots in the polymer chain may be mapped on to a more rugged energy landscape. In this scenario, the use of a stiff harmonic trap would result in the reduction of dissipation as the number of spring-dashpots are increased, or, as the landscape becomes more rugged. A thorough establishment of this connection on firmer mathematical grounds would involve the calculation of the work done in dragging a colloid over a rugged energy landscape, and examining its dependence on the stiffness of the harmonic trap used for the purpose. This exercise, while expected to be useful and instructive, is beyond the scope of the present work.

ACKNOWLEDGMENTS

R. K. thanks the Indian Institute of Technology Indore for supporting this work through the Young Faculty Research Grant Scheme (Project No. IITI/YFRSG/2024-2025/Phase-VII/01).

DATA AVAILABILITY STATEMENT

MATLAB codes used for generating the figures in this work are available freely on GitHub⁶⁹.

Appendix: Simplifications used in the derivation of work expression

This section contains the detailed steps pertaining to the simplification of equations that appear in the derivation of the work expression.

1. Simplifying the second term on the RHS of eq. (30)

Defining

$$I = \int_0^{\tau_m} d\tau \dot{\mathbf{h}}(\tau) \cdot \int_0^\tau d\tau' \mathbf{G}(\tau - \tau') \cdot \mathbf{D} \cdot \mathbf{h}(\tau') \quad (\text{A.1})$$

we start by simplifying the term within the square braces on the RHS of eq. (A.1). Noting that

$$\frac{d}{d\tau'} \{ \mathbf{G}(\tau - \tau') \} \cdot \mathbf{A}^{-1} = \mathbf{G}(\tau - \tau') \cdot \mathbf{D}, \quad (\text{A.2})$$

and integrating the inner integral in eq. (A.1) by parts, we may write

$$\int_0^\tau d\tau' \mathbf{G}(\tau - \tau') \cdot \mathbf{D} \cdot \mathbf{h}(\tau') = \mathbf{A}^{-1} \cdot \mathbf{h}(\tau) - \mathbf{G}(\tau) \cdot \mathbf{A}^{-1} \cdot \mathbf{h}(0) - \int_0^\tau d\tau' \mathbf{G}(\tau - \tau') \cdot \mathbf{A}^{-1} \cdot \dot{\mathbf{h}}(\tau') \quad (\text{A.3})$$

Substituting eq. (A.3) into eq. (A.1), we obtain

$$I = \int_0^{\tau_m} d\tau \dot{\mathbf{h}}(\tau) \cdot \mathbf{A}^{-1} \cdot \mathbf{h}(\tau) - \int_0^{\tau_m} d\tau \dot{\mathbf{h}}(\tau) \cdot \mathbf{G}(\tau) \cdot \mathbf{A}^{-1} \cdot \mathbf{h}(0) - \int_0^{\tau_m} d\tau \int_0^\tau d\tau' \dot{\mathbf{h}}(\tau) \cdot \mathbf{G}(\tau - \tau') \cdot \mathbf{A}^{-1} \cdot \dot{\mathbf{h}}(\tau') \quad (\text{A.4})$$

which, upon substitution into eq. (30), yields eq. (31).

2. Simplifying the second term on the RHS of eq. (31)

Defining

$$J = \int_0^{\tau_m} d\tau \dot{\mathbf{h}}(\tau) \cdot \mathbf{A}^{-1} \cdot \mathbf{h}(\tau) \quad (\text{A.5})$$

and integrating by parts, we get

$$\begin{aligned} J &= \mathbf{h}(\tau) \cdot \mathbf{A}^{-1} \cdot \mathbf{h}(\tau) \Big|_0^{\tau_m} - \int_0^{\tau_m} d\tau \dot{\mathbf{h}}(\tau) \cdot \mathbf{A}^{-1} \cdot \mathbf{h}(\tau) \\ &= \mathbf{h}(\tau_m) \cdot \mathbf{A}^{-1} \cdot \mathbf{h}(\tau_m) - \mathbf{h}(0) \cdot \mathbf{A}^{-1} \cdot \mathbf{h}(0) - J \end{aligned} \quad (\text{A.6})$$

and finally,

$$J = \frac{1}{2} [\mathbf{h}(\tau_m) \cdot \mathbf{A}^{-1} \cdot \mathbf{h}(\tau_m) - \mathbf{h}(0) \cdot \mathbf{A}^{-1} \cdot \mathbf{h}(0)] \quad (\text{A.7})$$

Substituting eq. (A.7) into eq. (31) and simplifying results in eq. (32).

3. Simplifying the second term on the RHS of eq. (40)

Noting that

$$\begin{aligned} &\mathbf{G}(\tau_1 - \tau'_2) \cdot \mathbf{G}(\tau_2 - \tau'_2) \\ &= \exp[-\mathbf{D} \cdot \mathbf{A}(\tau_1 - \tau'_2)] \exp[-\mathbf{D} \cdot \mathbf{A}(\tau_2 - \tau'_2)] \\ &= \exp[-\mathbf{D} \cdot \mathbf{A}(\tau_1 + \tau_2)] \exp[2\mathbf{D} \cdot \mathbf{A}\tau'_2], \end{aligned} \quad (\text{A.8})$$

we may write

$$\begin{aligned} \int_0^{\tau_2} d\tau'_2 \exp[2\mathbf{D} \cdot \mathbf{A}\tau'_2] &= \frac{1}{2} \mathbf{D}^{-1} \cdot \mathbf{A}^{-1} \exp[2\mathbf{D} \cdot \mathbf{A}\tau'_2] \Big|_0^{\tau_2} \\ &= \frac{1}{2} \mathbf{D}^{-1} \cdot \mathbf{A}^{-1} \exp[2\mathbf{D} \cdot \mathbf{A}\tau_2] - \frac{1}{2} \mathbf{D}^{-1} \cdot \mathbf{A}^{-1}, \end{aligned} \quad (\text{A.9})$$

we obtain the identity given in eq. (41). Using the identity to simplify the second term on the RHS of eq. (40) results in eq. (42).

¹W. Kuhn and H. Kuhn, "Bedeutung beschränkt freier Drehbarkeit für die Viskosität und Strömungsdoppelbrechung von Fadenmoleküllösungen I," *Helv. Chim. Acta* **28**, 1533–1579 (1945).

²H. C. Booij and P. H. van Wiechen, "Effect of Internal Viscosity on the Deformation of a Linear Macromolecule in a Sheared Solution," *J. Chem. Phys.* **52**, 5056–5068 (1970).

³C. W. Manke and M. C. Williams, "Stress Jump at the Inception of Shear and Elongational Flows of Dilute Polymer Solutions, Due to Internal Viscosity," *J. Rheol.* **31**, 495–510 (1987).

⁴C. C. Hua and J. D. Schieber, "Nonequilibrium Brownian dynamics simulations of Hookean and FENE dumbbells with internal viscosity," *J. Non-Newtonian Fluid Mech.* **56**, 307–332 (1995).

⁵C. C. Hua, J. D. Schieber, and C. W. Manke, "Linear viscoelastic behavior of the Hookean dumbbell with internal viscosity," *Rheol. Acta* **35**, 225–232 (1996).

⁶R. Kailasham, R. Chakrabarti, and J. R. Prakash, "Rheological consequences of wet and dry friction in a dumbbell model with hydrodynamic interactions and internal viscosity," *J. Chem. Phys.* **149**, 094903 (2018).

⁷M. E. Mackay, C. H. Liang, and P. J. Halley, "Instrument effects on stress jump measurements," *Rheol. Acta* **31**, 481–489 (1992).

⁸D. J. Massa, J. L. Schrag, and J. D. Ferry, "Dynamic Viscoelastic Properties of Polystyrene in High-Viscosity Solvents. Extrapolation to Infinite Dilution and High-Frequency Behavior," *Macromolecules* **4**, 210–214 (1971).

⁹A. Ansari, C. M. Jones, E. R. Henry, J. Hofrichter, and W. A. Eaton, "The Role of Solvent Viscosity in the Dynamics of Protein Conformational Changes," *Science* **256**, 1796–1798 (1992).

- ¹⁰G. S. Jas, W. A. Eaton, and J. Hofrichter, "Effect of Viscosity on the Kinetics of α -Helix and β -Hairpin Formation," *J. Phys. Chem. B* **105**, 261–272 (2001).
- ¹¹L. Qiu and S. J. Hagen, "A Limiting Speed for Protein Folding at Low Solvent Viscosity," *J. Am. Chem. Soc.* **126**, 3398–3399 (2004).
- ¹²T. Cellmer, E. R. Henry, J. Hofrichter, and W. A. Eaton, "Measuring internal friction of an ultrafast-folding protein," *Proc. Natl. Acad. Sci. U.S.A.* **105**, 18320–18325 (2008).
- ¹³S. J. Hagen, "Solvent viscosity and friction in protein folding dynamics," *Curr. Protein Pept. Sci.* **11**, 385–395 (2010).
- ¹⁴B. G. Wensley, S. Batey, F. A. C. Bone, Z. M. Chan, N. R. Tumelty, A. Steward, L. G. Kwa, A. Borgia, and J. Clarke, "Experimental evidence for a frustrated energy landscape in a three-helix-bundle protein family," *Nature* **463**, 685–688 (2010).
- ¹⁵A. Soranno, B. Buchli, D. Nettels, R. R. Cheng, S. Müller-Spáth, S. H. Pfeil, A. Hoffmann, E. A. Lipman, D. E. Makarov, and B. Schuler, "Quantifying internal friction in unfolded and intrinsically disordered proteins with single-molecule spectroscopy," *Proc. Natl. Acad. Sci. U.S.A.* **109**, 17800–17806 (2012).
- ¹⁶D. de Sancho, A. Sirur, and R. B. Best, "Molecular origins of internal friction effects on protein-folding rates," *Nat. Commun.* **5**, 4307 (2014).
- ¹⁷I. Echeverria, D. E. Makarov, and G. A. Papoian, "Concerted dihedral rotations give rise to internal friction in unfolded proteins," *J. Am. Chem. Soc.* **136**, 8708–8713 (2014).
- ¹⁸J. C. F. Schulz, M. S. Miettinen, and R. R. Netz, "Unfolding and Folding Internal Friction of β -Hairpins Is Smaller than That of α -Helices," *J. Phys. Chem. B* **119**, 4565–4574 (2015).
- ¹⁹N. Samanta and R. Chakrabarti, "Reconfiguration dynamics in folded and intrinsically disordered protein with internal friction: Effect of solvent quality and denaturant," *Physica A* **450**, 165–179 (2016).
- ²⁰A. Soranno, A. Holla, F. Dingfelder, D. Nettels, D. E. Makarov, and B. Schuler, "Integrated view of internal friction in unfolded proteins from single-molecule FRET, contact quenching, theory, and simulations," *Proc. Natl. Acad. Sci. U.S.A.* **114**, E1833–E1839 (2017).
- ²¹M. G. Poirier and J. F. Marko, "Effect of Internal Friction on Biofilament Dynamics," *Phys. Rev. Lett.* **88**, 228103 (2002).
- ²²Y. Murayama, H. Wada, and M. Sano, "Dynamic force spectroscopy of a single condensed DNA," *Eur. Phys. Lett.* **79**, 58001 (2007).
- ²³B. S. Khatri, M. Kawakami, K. Byrne, D. A. Smith, and T. C. B. McLeish, "Entropy and barrier-controlled fluctuations determine conformational viscoelasticity of single biomolecules," *Biophys. J.* **92**, 1825–1835 (2007).
- ²⁴A. Alexander-Katz, H. Wada, and R. R. Netz, "Internal friction and nonequilibrium unfolding of polymeric globules," *Phys. Rev. Lett.* **103**, 028102 (2009).
- ²⁵T. R. Einert, C. E. Sing, A. Alexander-Katz, and R. R. Netz, "Conformational dynamics and internal friction in homopolymer globules: Equilibrium vs. non-equilibrium simulations," *Eur. Phys. J. E* **34**, 130 (2011).
- ²⁶H. Ojala, G. Ziedaite, A. E. Wallin, D. H. Bamford, and E. Hægström, "Optical tweezers reveal force plateau and internal friction in PEG-induced DNA condensation," *Eur. Biophys. J.* **43**, 71–79 (2014).
- ²⁷D. Mondal, R. Adhikari, and P. Sharma, "Internal friction controls active ciliary oscillations near the instability threshold," *Sci. Adv.* **6**, eabb0503 (2020).
- ²⁸A. Nandagiri, A. S. Gaikwad, D. L. Potter, R. Nosrati, J. Soria, M. K. O'Bryan, S. Jadhav, and R. Prabhakar, "Flagellar energetics from high-resolution imaging of beating patterns in tethered mouse sperm," *eLife* **10**, e62524 (2021).
- ²⁹J. C. F. Schulz, L. Schmidt, R. B. Best, J. Dzubiella, and R. R. Netz, "Peptide Chain Dynamics in Light and Heavy Water: Zooming in on Internal Friction," *J. Am. Chem. Soc.* **134**, 6273–6279 (2012).
- ³⁰J. C. F. Schulz, M. S. Miettinen, and R. R. Netz, "Unfolding and Folding Internal Friction of β -Hairpins Is Smaller than That of α -Helices," *J. Phys. Chem. B* **119**, 4565–4574 (2015).
- ³¹P.-G. de Gennes, *Scaling Concepts in Polymer Physics* (Cornell University Press, Ithaca, 1979).
- ³²B. S. Khatri and T. C. B. McLeish, "Rouse model with internal friction: A coarse grained framework for single biopolymer dynamics," *Macromolecules* **40**, 6770–6777 (2007).
- ³³R. Kailasham, R. Chakrabarti, and J. R. Prakash, "Wet and dry internal friction can be measured with the Jarzynski equality," *Phys. Rev. Res.* **2**, 013331 (2020).
- ³⁴Z. Han, S. L. Hilburg, and A. Alexander-Katz, "Forced Unfolding of Protein-Inspired Single-Chain Random Heteropolymers," *Macromolecules* **55**, 1295–1309 (2022).
- ³⁵M. Fixman, "Dynamics of stiff polymer chains," *J. Chem. Phys.* **89**, 2442 (1988).
- ³⁶J. O. Daldrop, J. Kappler, F. N. Brunig, and R. R. Netz, "Butane dihedral angle dynamics in water is dominated by internal friction," *Proc. Natl. Acad. Sci. U.S.A.* **115**, 5169–5174 (2018).
- ³⁷A. Świątek, K. Kuczera, and R. Szoszkiewicz, "Effects of Proline on Internal Friction in Simulated Folding Dynamics of Several Alanine-Based α -Helical Peptides," *J. Phys. Chem. B* **128**, 3856–3869 (2024).
- ³⁸T. P. Dasbach, C. W. Manke, and M. C. Williams, "Complex viscosity for the rigorous formulation of the multibead internal viscosity model with hydrodynamic interaction," *J. Phys. Chem.* **96**, 4118–4125 (1992).
- ³⁹R. Kailasham, R. Chakrabarti, and J. R. Prakash, "Rouse model with fluctuating internal friction," *J. Rheol.* **65**, 903 (2021).
- ⁴⁰R. Kailasham, R. Chakrabarti, and J. R. Prakash, "Shear viscosity for finitely extensible chains with fluctuating internal friction and hydrodynamic interactions," *J. Rheol.* **67**, 105–123 (2023).
- ⁴¹H. C. Öttinger, *Stochastic Processes in Polymeric Fluids* (Springer, Berlin, 1996).
- ⁴²R. B. Bird, C. F. Curtiss, R. C. Armstrong, and O. Hassager, *Dynamics of Polymeric Liquids - Volume 2 : Kinetic Theory* (John Wiley and Sons, New York, 1987).
- ⁴³A. Dhar, "Work distribution functions in polymer stretching experiments," *Phys. Rev. E* **71**, 036126 (2005).
- ⁴⁴T. Speck and U. Seifert, "Dissipated work in driven harmonic diffusive systems: General solution and application to stretching Rouse polymers," *Eur. Phys. J. B* **43**, 521–527 (2005).
- ⁴⁵A. Varghese, S. Vemparala, and R. Rajesh, "Force fluctuations in stretching a tethered polymer," *Phys. Rev. E* **88**, 022134 (2013).
- ⁴⁶J. R. Prakash, "The kinetic theory of dilute solutions of flexible polymers: Hydrodynamic interaction," in *Rheology Series*, Vol. 8, edited by D. A. Siginer, D. De Kee, and R. P. Chhabra (Elsevier, 1999) pp. 467–517.
- ⁴⁷C. Jarzynski, "Nonequilibrium Equality for Free Energy Differences," *Phys. Rev. Lett.* **78**, 2690–2693 (1997).
- ⁴⁸M. T. Woodside and S. M. Block, "Reconstructing Folding Energy Landscapes by Single-Molecule Force Spectroscopy," *Ann. Rev. Biophys.* **43**, 19–39 (2014).
- ⁴⁹J. Liphardt, S. Dumont, S. B. Smith, I. Tinoco Jr., and C. Bustamante, "Equilibrium information from nonequilibrium measurements in an experimental test of Jarzynski's equality," *Science* **296**, 1832–1835 (2002).
- ⁵⁰O. Braun, A. Hanke, and U. Seifert, "Probing molecular free energy landscapes by periodic loading," *Phys. Rev. Lett.* **93**, 158105 (2004).
- ⁵¹P. Szymczak and H. Janovjak, "Periodic Forces Trigger a Complex Mechanical Response in Ubiquitin," *J. Mol. Biol.* **390**, 443–456 (2009).
- ⁵²M. Wu and H. P. Lu, "Oscillating Piconewton Force Manipulation on Single-Molecule Enzymatic Conformational and Reaction Dynamics," *J. Phys. Chem. B* **122**, 12312–12321 (2018).
- ⁵³T. Speck and U. Seifert, "Distribution of work in isothermal nonequilibrium processes," *Phys. Rev. E* **70**, 066112 (2004).
- ⁵⁴H. B. Callen, *Thermodynamics and an Introduction to Thermostatistics* (John Wiley and Sons, New York, 1985).

- ⁵⁵J. N. Onuchic, Z. Luthey-Schulten, and P. G. Wolynes, "Theory of protein folding: the energy landscape perspective," *Annu. Rev. Phys. Chem.* **48**, 545–600 (1997).
- ⁵⁶R. Zwanzig, "Diffusion in a rough potential," *Proc. Natl. Acad. Sci. U.S.A.* **85**, 2029–2030 (1988).
- ⁵⁷S. Park, F. Khalili-Araghi, E. Tajkhorshid, and K. Schulten, "Free energy calculation from steered molecular dynamics simulations using Jarzynski's equality," *J. Chem. Phys.* **119**, 3559–3566 (2003).
- ⁵⁸S. Park and K. Schulten, "Calculating potentials of mean force from steered molecular dynamics simulations," *J. Chem. Phys.* **120**, 5946–5961 (2004).
- ⁵⁹D. D. Minh and J. Andrew McCammon, "Springs and speeds in free energy reconstruction from irreversible single-molecule pulling experiments," *J. Phys. Chem. B* **112**, 5892–5897 (2008).
- ⁶⁰S. Blaber and D. A. Sivak, "Efficient two-dimensional control of barrier crossing," *Epl* **139**, 17001 (2022).
- ⁶¹S. Blaber and D. A. Sivak, "Optimal control with a strong harmonic trap," *Phys. Rev. E* **106**, L022103 (2022).
- ⁶²F. Latinwo and C. M. Schroeder, "Nonequilibrium work relations for polymer dynamics in dilute solutions," *Macromolecules* **46**, 8345–8355 (2013).
- ⁶³F. Latinwo, K.-W. Hsiao, and C. M. Schroeder, "Nonequilibrium thermodynamics of dilute polymer solutions in flow," *J. Chem. Phys.* **141**, 174903 (2014).
- ⁶⁴F. Latinwo and C. M. Schroeder, "Determining elasticity from single polymer dynamics," *Soft matter* **10**, 2178–87 (2014).
- ⁶⁵Y. Zhou, F. Latinwo, and C. M. Schroeder, "Crooks fluctuation theorem for single polymer dynamics in time-dependent flows: Understanding viscoelastic hysteresis," *Entropy* **24**, 27 (2022).
- ⁶⁶A. Ghosal and B. J. Cherayil, "Polymer extension under flow: Some statistical properties of the work distribution function," *J. Chem. Phys.* **145**, 204901 (2016).
- ⁶⁷R. Sharma and B. J. Cherayil, "Work fluctuations in an elastic dumbbell model of polymers in planar elongational flow," *Phys. Rev. E* **83**, 1–8 (2011).
- ⁶⁸A. Ghosal and B. J. Cherayil, "Polymer extension under flow: A path integral evaluation of the free energy change using the Jarzynski relation," *J. Chem. Phys.* **144** (2016).
- ⁶⁹R. Kailasham, "MATLAB codes for calculating dissipation in driven bead-spring-dashpot chains," (2025), https://github.com/rkailasham/bsp_dashpot_lin_sym_driving.